



**ISEL**



**ESCOLA SUPERIOR DE  
TECNOLOGIA DA SAÚDE  
DE LISBOA**

## **Impact of centrosome amplification in the malignant transformation of Barrett's Esophagus**

**BÁRBARA NUNES AMARAL DA SILVA SILVEIRA**  
(Licenciada)

Dissertação para obtenção do grau de Mestre em Engenharia Biomédica

Orientadores:

Doutora Cecília Ribeiro da Cruz Calado

Doutora Carla Alexandra Mendes Lopes

Júri:

Presidente: Doutor Paulo Jorge Leitão Pessoa Guerreiro

Vogais:

Doutora Sandra Raquel Oliveira Tavares

Doutora Carla Alexandra Mendes Lopes

**Setembro de 2024**



# **Impact of centrosome amplification in the malignant transformation of Barrett's Esophagus**

**BÁRBARA NUNES AMARAL SILVA SILVEIRA**  
(Licenciada)

Dissertação para obtenção do grau de Mestre em Engenharia Biomédica

**Orientadores:**

Doutora Cecília Ribeiro da Cruz Calado, Instituto Superior de Engenharia de Lisboa

Doutora Carla Alexandra Mendes Lopes, Instituto Português de Oncologia de Lisboa Francisco Gentil

**Júri:**

Presidente: Doutor Paulo Jorge Leitão Pessoa Guerreiro, Escola Superior de Tecnologia da Saúde de Lisboa

**Vogais:**

Doutora Sandra Raquel Oliveira Tavares, Instituto de Investigação e Inovação em Saúde

Doutora Carla Alexandra Mendes Lopes, Instituto Português de Oncologia de Lisboa Francisco Gentil E.P.E.

**Setembro de 2024**



## Acknowledgments

This thesis represents the culmination of a journey made possible through the invaluable contributions of numerous individuals and institutions.

My deepest gratitude goes to my mentor, Dr. Carla A.M. Lopes, whose unwavering support, patience, and insightful guidance were instrumental in shaping this work. Her vast knowledge and dedication inspired me to strive for excellence and expand my research horizons. I am equally grateful to Dr. Cecília Calado for her collaborative spirit and willingness to embrace new research avenues.

I extend my sincere appreciation to the entire integrative Grupo de Estudo do Esófago de Barrett (GEEB) for their invaluable guidance and technical expertise.

I am particularly thankful to PhD. Marta Sirgado and PhD. Fernanda Silva, along with my former colleagues at IPOLFG, for their camaraderie. To all the support and understanding during the challenging times of my current colleagues at IMP diagnostics.

This research was made possible through the generous funding provided by the Liga Portuguesa Contra o Cancro – Núcleo Regional do Sul, through the research Fellowship LPCC-NRS/Terry Fox (TF 2022-24 CL). I am also grateful to the Instituto Português de Oncologia de Lisboa Francisco Gentil E.P.E. and the Instituto Gulbenkian de Ciência for providing the necessary resources and facilities to conduct this work.

Finally, my heartfelt gratitude goes to my family, whose unwavering love, patience, and encouragement have been my constant source of strength. My husband's daily support, especially during my absences, and his firm belief in my abilities fueled my determination to complete this project.

To my daughter, born during the course of this thesis, your arrival brought immeasurable joy and purpose to my life. Balancing motherhood and academia presented unique challenges, but it has been the most rewarding chapter of this journey.

It is with immense gratitude that I dedicate this work to all of you who have made this accomplishment possible.



## Statement of integrity

I declare that this dissertation is the result of my personal and independent research. Its content is original, and all sources listed in the bibliographic references were consulted and are duly mentioned in the text. I further declare that all scientific and technical references relevant to the development of the work are duly cited and included in the bibliographic references.

The author

Barbara N.A.S. Silveira  
Lisbon, 24<sup>th</sup> September 2024



# Impact of centrosome amplification in the malignant transformation of Barrett's Esophagus

## Resumo

O esófago de Barrett (EB) é uma condição pré-maligna de várias etapas, que progride de metaplasia para displasia e, finalmente, para adenocarcinoma esofágico. A detecção precoce do EB, bem como a estratificação do seu risco de progressão, está a tornar-se uma preocupação crescente. A amplificação dos centrossomas (AC) é observada em células metaplásicas de EB e aumenta ao longo da progressão, particularmente de metaplasia para displasia. Dado que a AC é descrita em vários cancros humanos e pode contribuir para o desenvolvimento de malignidade, colocámos a hipótese de que a AC pode promover a progressão maligna do EB, influenciando o potencial de migração e invasão das células displásicas. A redução da AC em displasia poderia, assim, diminuir o potencial invasivo destas células. Ao reduzir o nível de AC através da depleção de moléculas da biogénese centriolar, observámos uma diminuição do potencial migratório e invasivo das células displásicas. A transição epitelial-mesenquimal (EMT), frequentemente associada à malignidade e invasão, foi também investigada. Questionámos se a redução da AC poderia reverter a EMT, aumentando características epiteliais e reduzindo as mesenquimais, responsáveis pelo potencial migratório e invasivo das células. Embora a redução da AC nas células displásicas não tenha provocado mudanças significativas na assinatura de EMT, levou à acumulação citosólica de um componente da matriz extracelular, acompanhada por níveis reduzidos desse componente no espaço extracelular. Os nossos resultados indicam que a AC contribui para o potencial invasivo na displasia e fornecem pistas importantes sobre os seus mecanismos. Este estudo fornece novas informações sobre o papel dos centrossomas supranumerários na progressão maligna do EB e poderá ajudar no desenvolvimento de novos biomarcadores de progressão, além de possibilitar uma terapia mais personalizada.

**Palavras-chave:** Esófago de Barrett, Amplificação de Centrossomas, Progressão tumoral, Invasão.



# Impact of centrosome amplification in the malignant transformation of Barrett's Esophagus

## Abstract

Barrett's esophagus (BE) is a multistep premalignant condition, progressing from metaplasia, dysplasia, to, ultimately, esophageal adenocarcinoma (EAC). BE early detection, as well as stratifying its risk of progression, is becoming a growing concern. Centrosome amplification (CA) is observed in metaplastic BE cells and increases throughout progression, significantly increasing from metaplasia to dysplasia. Because CA has been described in many human cancers and may contribute to the development of malignancy, we hypothesized that CA may contribute to BE malignant progression by impacting the migration and invasion potentials of BE dysplastic cells. If this hypothesis is correct, a decrease of CA in dysplasia would be sufficient to reduce malignant properties such as invasiveness potential. Indeed, by depleting molecules of centriolar biogenesis to reduce the level of CA, we observed a reduced migratory and invasive potential of dysplastic cells. As epithelial-mesenchymal transition (EMT) is often linked to malignancy and invasion capacity, we investigated whether the reduction of extra centrosomes could result in an EMT reversal, increasing epithelial cellular traits and lessening mesenchymal features responsible for the migratory and invasive potential of the cells. Although the reduction of CA in dysplasia cells was not accompanied by significant changes in their EMT signature, there was a cytosolic accumulation of a component of the extracellular matrix. Notably, this was accompanied by reduced levels of this component in the extracellular space. In summary, our results indicate that CA contributes to the invasive potential in dysplasia and provides important clues into their mechanisms. This study provides new insights regarding the contribution of supernumerary centrosomes to the invasive potential in dysplasia, highlighting the importance of CA in the malignant progression of BE. These findings may contribute to the development of new biomarkers of progression and personalizing therapy.

**Keywords:** Barrett's esophagus, Centrosome Amplification, Tumor Progression, Invasion.



# Table of Contents

<b>ACKNOWLEDGMENTS</b> .....	<b>I</b>
<b>STATEMENT OF INTEGRITY</b> .....	<b>III</b>
<b>RESUMO</b> .....	<b>V</b>
<b>ABSTRACT</b> .....	<b>VII</b>
<b>TABLE OF CONTENTS</b> .....	<b>IX</b>
<b>LIST OF FIGURES</b> .....	<b>XI</b>
<b>LIST OF TABLES</b> .....	<b>XI</b>
<b>LIST OF ABBREVIATIONS</b> .....	<b>XII</b>
<b>1. INTRODUCTION</b> .....	<b>1</b>
1.1 BARRETT’S ESOPHAGUS (BE): A CANCER PRECURSOR .....	1
1.1.1 <i>BE definition, diagnosis, and pathogenesis</i> .....	1
1.1.2 <i>BE malignant progression</i> .....	2
1.1.3 <i>Management of BE patients: need for biomarkers</i> .....	4
1.1.4 <i>Using BE Progression as a Tumorigenesis Model</i> .....	5
1.2 CENTROSOMES.....	5
1.2.1 <i>Centrosome structure and function</i> .....	6
1.2.2 <i>The centrosome duplication cycle</i> .....	8
1.3 CENTROSOME DEREGLATION AND CANCER .....	10
1.3.1 <i>Causes and consequences of centrosome amplification</i> .....	10
1.3.2 <i>Centrosome amplification and cell invasion</i> .....	12
1.4 CENTROSOME AMPLIFICATION AND BARRETT’S ESOPHAGUS TUMORIGENESIS .....	13
1.5 CENTROSOME AMPLIFICATION, EMT CHANGES, AND BE PROGRESSION.....	15
1.5.1 <i>Vimentin and Fibronectin</i> .....	16
1.6 AIMS AND OBJECTIVES .....	18
<b>2. MATERIAL AND METHODS</b> .....	<b>19</b>
2.1 CELL CULTURE .....	19
2.1.1 <i>Cell line maintenance</i> .....	19
2.1.2 <i>siRNA transfection</i> .....	19
2.1.3 <i>Cell Viability Assessment</i> .....	20
2.1.4 <i>Transwell migration and invasion assays</i> .....	20
2.2 RT-QPCR.....	20

2.3	WESTERN BLOT .....	21
2.3.1	<i>Cell lysis, SDS-PAGE and transfer</i> .....	21
2.3.2	<i>Protein detection</i> .....	22
2.4	IMMUNOFLUORESCENCE MICROSCOPY .....	22
2.4.1	<i>Cell fixation</i> .....	22
2.4.2	<i>Immunofluorescent staining</i> .....	22
2.4.3	<i>Antibodies</i> .....	23
2.4.4	<i>Image Analysis</i> .....	23
2.4.5	<i>Centriole Count</i> .....	23
2.4.6	<i>Analysis of EMT Markers</i> .....	23
2.5	ENZYME-LINKED IMMUNOSORBENT ASSAY (ELISA) .....	24
2.6	STATISTICAL ANALYSIS .....	24
<b>3.</b>	<b>RESULTS .....</b>	<b>24</b>
3.1	THE IMPACT OF REDUCING CA IN THE MIGRATORY AND INVASIVENESS CAPACITY OF DYSPLASIA CELLS .....	25
3.1.1	<i>Depletion of PLK4 or SAS6 leads to a significant decrease of CA in dysplasia cells</i> .....	26
3.1.2	<i>Reduction of CA levels decreases the migratory and invasive capacity of dysplasia cells</i> .....	28
3.2	THE IMPACT OF REDUCING CA IN THE EMT FEATURES OF DYSPLASIA CELLS.....	29
3.2.1	<i>Global mRNA and protein levels of EMT markers upon CA reduction</i> .....	29
3.2.2	<i>Analysis of the impact of CA reduction in EMT markers by IF</i> .....	31
3.3	THE IMPACT OF REDUCING CA ON FIBRONECTIN AND ITS ROLE IN CELL INVASION	34
3.3.1	<i>Impact of CA reduction on fibronectin secretion into extracellular space</i> ....	35
3.3.2	<i>Impact of reducing fibronectin secretion in dysplasia cells' migratory and invasiveness capacity</i> .....	35
<b>4.</b>	<b>DISCUSSION.....</b>	<b>37</b>
<b>5.</b>	<b>CONCLUSION AND FUTURE PERSPECTIVES .....</b>	<b>42</b>
<b>6.</b>	<b>REFERENCES.....</b>	<b>43</b>

## List of Figures

FIGURE 1.1 - BARRETT'S ESOPHAGUS ESTABLISHMENT AND ITS MALIGNANT PROGRESSION.	3
FIGURE 1.2 - THE CENTROSOME. ....	6
FIGURE 1.3 - THE CENTROSOME DUPLICATION CYCLE.....	8
FIGURE 1.4 - CONSEQUENCES OF CENTROSOME AMPLIFICATION IN CANCER.. ....	11
FIGURE 1.5 - CA CAN PROMOTE INVASIVE PHENOTYPES.. ....	12
FIGURE 1.6 - BARRETT'S ESOPHAGUS PROGRESSION AND CENTROSOME AMPLIFICATION. .	14
FIGURE 3.1 - SCHEMATIC REPRESENTATION OF THE EXPERIMENTAL LAYOUT.....	25
FIGURE 3.2 - DEPLETION OF KEY PROTEINS FOR CENTROSOME FORMATION REDUCES LEVELS OF CENTROSOME AMPLIFICATION (CA) IN DYSPLASIA CELLS.. ....	26
FIGURE 3.3 - DYSPLASIA CELLS' MIGRATION AND INVASION CAPACITY LESSENS WITH THE DECREASE OF CA LEVELS.....	28
FIGURE 3.4 - DYSPLASIA CELLS WITH REDUCED CA LEVELS EXHIBIT A HYBRID EMT PHENOTYPE. ....	30
FIGURE 3.5 - IMPACT OF CA REDUCTION ON E-CADHERIN. ....	31
FIGURE 3.6 - IMPACT OF CA REDUCTION ON VIMENTIN.....	32
FIGURE 3.7 - DEPLETION OF FIBRONECTIN IN DYSPLASIA CELLS.....	33
FIGURE 3.8 - IMPACT OF CA REDUCTION ON FIBRONECTIN.....	34
FIGURE 3.9 - DYSPLASIA CELLS SHOW DECREASED FIBRONECTIN SECRETION UPON CA REDUCTION.....	35
FIGURE 3.10 - DYSPLASIA CELLS' INVASION CAPACITY LESSENS WITH THE DEPLETION OF FIBRONECTIN.. ....	36

## List of Tables

TABLE 1.1 - CENTROSOMES FUNCTIONS.....	7
TABLE 2.1 - PRIMER SEQUENCES USED IN THE RT-QPCR.....	21

## List of Abbreviations

<b>BE</b>	<b>Barrett's Esophagus</b>
<b>BPE</b>	<b>Bovine pituitary extract</b>
<b>BSA</b>	<b>Bovine serum albumin</b>
<b>CA</b>	<b>Centrosome amplification</b>
<b>CIN</b>	<b>Chromosomal instability</b>
<b>CP-D</b>	<b>High-grade dysplastic Barrett's epithelial cell line D</b>
<b>DNA</b>	<b>Deoxyribonucleic acid</b>
<b>EAC</b>	<b>Esophageal Adenocarcinoma</b>
<b>ECASP</b>	<b>Extra centrosome-associated secretory phenotype</b>
<b>ECM</b>	<b>Extracellular matrix</b>
<b>ELISA</b>	<b>Enzyme-linked immunosorbent assay</b>
<b>EMT</b>	<b>Epithelial-to-mesenchymal transition</b>
<b>ESCC</b>	<b>Esophageal squamous cell carcinoma</b>
<b>FN1</b>	<b>Fibronectin 1</b>
<b>FBS</b>	<b>Fetal Bovine Serum</b>
<b>GERD</b>	<b>Gastroesophageal reflux disease</b>
<b>H&amp;E</b>	<b>Hematoxylineosin</b>
<b>HGD</b>	<b>High-grade dysplasia</b>
<b>IF</b>	<b>Immunofluorescence</b>
<b>LGD</b>	<b>Low-grade dysplasia</b>
<b>IM</b>	<b>Intestinal metaplasia</b>
<b>mRNA</b>	<b>Messenger RNA</b>
<b>MTs</b>	<b>Microtubules</b>
<b>MMPs</b>	<b>Matrix metalloproteinases</b>
<b>PCM</b>	<b>Pericentriolar material</b>
<b>PBS</b>	<b>Phosphate Buffered Saline</b>
<b>PLK4</b>	<b>Polo-like kinase 4</b>
<b>RT</b>	<b>Room temperature</b>
<b>RT-qPCR</b>	<b>Reverse transcriptase quantitative real-time polymerase chain reaction</b>
<b>ROS</b>	<b>Reactive oxygen species</b>
<b>RNA</b>	<b>Ribonucleic acid</b>
<b>SAS6</b>	<b>Spindle assembly abnormal protein homolog 6</b>
<b>TMEs</b>	<b>Tumor microenvironments</b>

*“O sucesso é a soma de pequenos esforços repetidos diariamente.”*

*Robert Collier (1885-1950).*

# 1. Introduction

Cancer research has made remarkable strides in recent years. A significant factor contributing to this progress is the exploration of the disparities between normal cells and tumor cells, which has led to the identification of specific molecules known as biomarkers. These biomarkers serve as valuable tools in detecting, managing, and preventing diseases, including all types of cancer.

## 1.1 Barrett's esophagus (BE): a cancer precursor

Barrett's Esophagus (BE) is a pre-malignant condition that can lead to tumor initiation<sup>1</sup>. Although the incidence of BE in the general population is estimated to be around 2%, it is more common in people with chronic gastroesophageal reflux disease (GERD)<sup>2</sup>. The significance of BE lies in its potential to develop into esophageal adenocarcinoma (EAC). The risk increases in the presence of dysplasia, whereas in high-grade dysplasia (HGD) cases, the progression rate is significantly higher, ranging from 7% to 10% per year<sup>2-4</sup>.

### 1.1.1 BE definition, diagnosis, and pathogenesis

The esophagus is a tubular structure composed of organized tissue layers, wherein intricate cellular networks work synergistically to facilitate the safe passage of nutrients and shield against the harsh gastric contents<sup>5</sup>. The usual lining of the esophagus consists of (i) a non-keratinizing stratified squamous epithelium; (ii) *lamina propria*, which is a layer of connective tissue that includes glands secreting neutral mucins to protect the esophagus from stomach acid; and (iii) a deeper layer of smooth muscle fibers oriented longitudinally, the *muscularis mucosae*.

Barrett's esophagus (BE) is a metaplastic transformation in which the original squamous epithelium is replaced by a columnar epithelium with gastric and intestinal characteristics, usually occurring in the lower esophagus near the gastroesophageal junction (JEG)<sup>6</sup>. Although the morphology of BE had been previously described by others, this condition was named after Norman Barrett, who reported in 1950 a case of chronic peptic ulcer in the lower esophagus covered by columnar epithelium<sup>7</sup>.

Today, for the American College of Gastroenterology (ACG) 2022, BE is “an extension of salmon-colored mucosa into the tubular esophagus extending  $\geq 1$  cm proximal to the gastroesophageal junction with biopsy confirmation of intestinal metaplasia (goblet cells)”<sup>8</sup>, and The British Society of Gastroenterology 2014 defined BE as a “columnar epithelium with or without goblet cells extending  $\geq 1$  cm proximal to the gastroesophageal junction”<sup>9</sup>.

The diagnosis of Barrett's esophagus has three important components: i) it is secondary to long-standing gastroesophageal reflux disease<sup>5</sup>; ii) there is an endoscopic (abnormal mucosa  $\geq 1$  cm proximal to the GE junction<sup>10</sup>) and histological (metaplastic epithelium<sup>8</sup>) correlation; and iii) the requirement of intestinal metaplasia for the diagnosis of BE varies, as it is mandatory in the USA and parts of Europe but not necessary in the UK and Japan<sup>8,9</sup>.

Gastroesophageal reflux disease (GERD) is a common inflammatory cause of BE and erosive esophagitis. It occurs when stomach acid repeatedly flows back into the esophagus. This acid backwash can irritate the lining of the esophagus, creating inflammation<sup>7,11</sup>.

Research in the pathogenesis of BE has two main branches, one focusing on the location and identity of the cell origin and the other on cell replacement mechanisms<sup>1,12</sup>. Regarding the original location and identity, it is hypothesized that the origin cell is native to the esophagus (squamous cells, ductal cells, and submucosal gland cells), cells located at the squamocolumnar junction (transitional basal cells and embryonic stem cells), cells from the proximal stomach (gastric cardia), or even bone marrow-derived cells<sup>1</sup>. In the attempt to elucidate the mechanism of cell replacement, there has been research about transdifferentiation (transformation of one differentiated cell type to another) or trans-commitment (reprogramming at the stem or progenitor cell level)<sup>6,13,14</sup>.

### **1.1.2 BE malignant progression**

There is abundant evidence that adenocarcinoma in the setting of Barrett's esophagus develops through a progressive sequence of histological and molecular events.<sup>14–16</sup> BE malignant transformation is a multistep process from metaplasia (pre-malignant condition) to dysplasia (intraepithelial neoplasia), adenocarcinoma (invasive neoplasia), and metastasis (Figure 1.1).

The presence of dysplasia cells (abnormal cells) within BE metaplasia leads to its reclassification as low-grade dysplasia (LGD) or high-grade dysplasia (HGD), depending on cytological and architectural changes like cellular alignment and nuclear polarity. HGD is termed *Tumour in situ*<sup>17</sup> if the basement membrane confines malignant cells. In esophageal adenocarcinoma (EAC), the neoplastic cells go beyond the epithelium and infiltrate the *lamina propria*, the *muscularis mucosa*, and/or submucosa<sup>17</sup>. This often causes a desmoplastic reaction<sup>18</sup>. Along with changes in the surface cells, there are also mesenchymal and stromal alterations. The *lamina propria* commonly has increased blood and lymphatic vessels, as well as nerve fibers, and displays features associated with chronic inflammation. The *muscularis mucosae* is also rearranged (duplication), usually with a thick single or double-layer<sup>15</sup>.

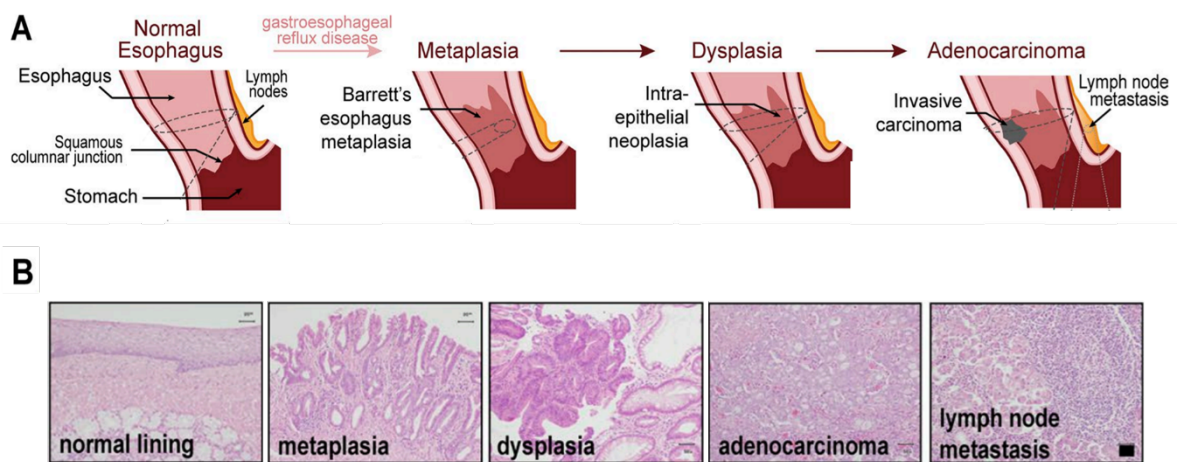


**Figure 1.1 - Barrett's Esophagus establishment and its malignant progression.** (A) Schematic anatomical representation of Barrett's esophagus progression from metaplasia to dysplasia, adenocarcinoma, and metastasis. (B) Histologic representation of neoplastic evolution (Adapted from Lopes et al., 2018).

The length of the Barrett's esophagus segment, presence of dysplasia (especially high-grade), tobacco use, central obesity, older age, caucasian, male sex, and erosive esophagitis are all associated with a higher risk of progression to esophageal adenocarcinoma in patients with Barrett's esophagus<sup>19</sup>. These factors highlight the importance of close monitoring and appropriate management strategies for patients at risk of progressing to cancer<sup>2,7,11</sup>.

At the molecular level, Barrett's esophagus carcinogenesis is characterized by loss of heterozygosity (LOH), aneuploidy, specific genetic mutations, and clonal diversity<sup>16</sup>. For example, DNA methylation resulting in loss of p16 expression and loss of wild-type p53 function in metaplasia to dysplasia transition are known common molecular

changes<sup>16,20-22</sup>. However, the specific molecular events that underlie the pathogenesis of BE carcinogenesis are still unknown. The progression of BE towards malignancy, while continuous and cumulative, is not linear<sup>21</sup>. It holds a large spectrum of alterations that spans from metaplasia stage (pre-malignant) to LGD/HGD stages (intra-epithelial neoplasia) to EAC (invasive neoplasia) at several levels. Some patients can experience a faster progression towards malignancy, which reduces the time available to detect cancer at an early stage<sup>21</sup>. Its multifaceted, complex origin may originate from this<sup>1,23</sup>. As the precise mechanisms underlying BE progression to esophageal adenocarcinoma remain poorly understood, there is a need for identifiable metaplastic precursors to enable early detection of malignant transformation<sup>8,23</sup>.

### **1.1.3 Management of BE patients: need for biomarkers**

Although BE poses a high risk for EAC, a type of cancer with an extremely poor prognosis, it is not certain that people with BE progress to cancer<sup>7,8</sup>.

Patients with BE are largely undiagnosed, so the overall prevalence is difficult to define. In patients suffering from GERD but otherwise well, it can be seen in up to 15% of cases<sup>3,4</sup>. Once the first biopsy makes the diagnosis, patients are monitored by regular endoscopy screening and generally with more following biopsies. The histologic assessment on the hematoxylin-eosin (H&E) slide remains the gold standard for diagnosing dysplasia and cancer<sup>8</sup>. The frequency of testing will depend on the results of the last biopsy<sup>8,9</sup>. After confirming dysplasia, the patient's surveillance is tighter, and clinical treatment options are available. Other methods of detecting progression include chromoendoscopy, narrow-band imaging, and autofluorescence endoscopy<sup>11</sup>. It has been found that only a small percentage, between 0.1% and 0.5%, of patients with BE findings will develop neoplasia in a year<sup>24</sup>. However, once dysplasia is detected, there is a synergistic effect between BE and EAC. This highlights the connection between the two and the need for better diagnostic methods for patients<sup>8,11,25</sup>.

BE early detection, as well as stratifying its risk of progression, is becoming a growing concern<sup>19,25,26</sup>. Key strategies to significantly lower the occurrence and death rates associated with esophageal adenocarcinoma include early screening, prompt diagnosis, and timely treatment. Expanding knowledge about disease onset in every aspect - endoscopic, molecular, pathologic, and epidemiologic - is imperative.

At the molecular level, identifying biomarkers for progression in this pre-malignant condition could be a turning point in preventing EAC and managing it globally. Our laboratory work has focused on identifying progression biomarkers using Barrett's esophagus carcinogenesis as a cancer model.

#### **1.1.4 Using BE Progression as a Tumorigenesis Model**

BE has been serving as a model for tumor growth analysis<sup>20</sup>, as it comprises all stages of the disease and depicts its multistep evolution toward malignancy<sup>14,21</sup>.

The knowledge obtained specifically from the *in vitro* models can cover the esophageal non-cancerous lining to the beginning of cancer and its late stages<sup>27-29</sup>. As a result, several events that occur in cancer development can be explored, such as chronic inflammation, epithelial-to-mesenchymal (EMT) transition, migration and invasion, and cellular signaling alterations. If properly explored, all these findings can significantly impact tracking and stratifying the risk of patients developing EAC. Various preclinical models have been developed to study BE, including *in vivo* (murine and dog) and *in vitro* models (cell culture and organotypic or organoids)<sup>20</sup>. Each model has advantages and disadvantages, making it challenging to identify a single ideal model for studying Barrett's carcinogenesis. While significant progress has been made in developing preclinical models for Barrett's esophagus, challenges remain in achieving models that accurately reflect the human condition and can be effectively used for therapeutic testing.

## **1.2 Centrosomes**

The centrosome is the major microtubule organizing center (MTOC) in animal cells. It is responsible for the spatial organization of microtubules (MTs), which, together with intermediate filaments and actin microfilaments, constitute the cytoskeleton<sup>30,31</sup>.

Theodore Boveri was not the first to describe the centrosome, but his studies in roundworm *Ascaris*, made major advancements in understanding the cell-division cycle<sup>32,33</sup>. In 1887, Boveri distinctly described two cycles, the chromosome cycle and the centrosome cycle, which are closely synchronized but can occur independently. He described centrosomes as the proper cell division centers in each cell cycle mitoses and that centrosome duplication and DNA replication are initiated at about the same

time at interphase<sup>33</sup>. Boveri minutely depicted the centrosome cycle, uncovering that centrosomes can self-replicate and are inherited by daughter cells. He defined the centrosome as a key organelle that organizes cellular division, being essential for mitotic spindle formation during cell division. Additionally, he hinted about the role of the centrosome in cancer, speculating that chromosome aneuploidy, induced by extra centrosomes, was a principal cause of cancer<sup>33</sup>.

Boveri's work laid the groundwork for our current understanding of the centrosome structure and function, influencing developmental biology and our understanding of cellular organization<sup>32</sup>. Recently, centrosomes returned to the focus of research due to their roles in cellular homeostasis<sup>34</sup>. Notably, centrosome abnormalities have been detected in several human cancers and are considered a hallmark of cancer<sup>35-38</sup>

### 1.2.1 Centrosome structure and function

In animal cells, the centrosome is a non-membranous organelle that comprises a pair of centrioles arranged in orthogonal order surrounded by an electron-dense matrix, the pericentriolar material (PCM)<sup>39,40</sup> (Figure 1.2).

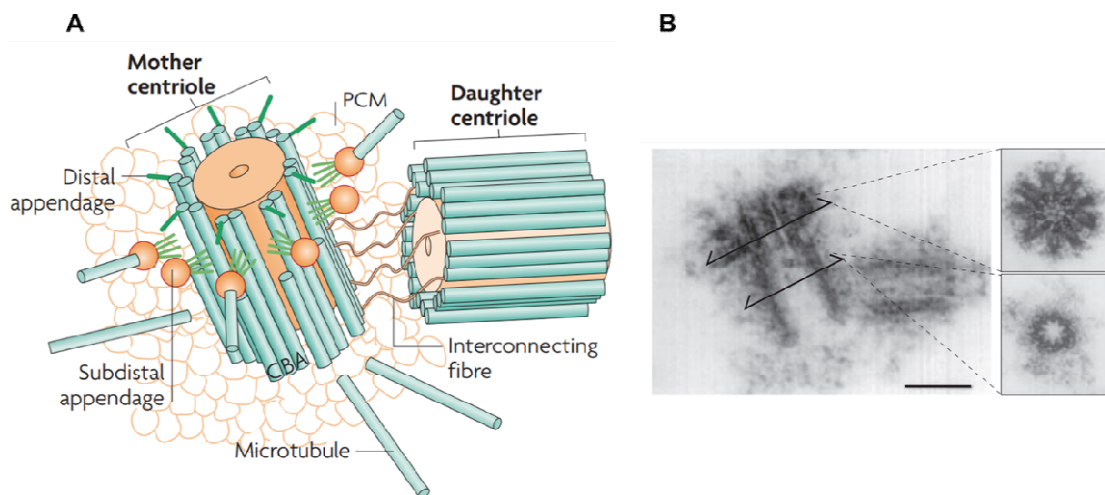


**Figure 1.2 - The centrosome.** (A) Schematic representation of the centrosome in animal cells. The centrosome comprises two MT-based centrioles surrounded by a dense and highly structured mass of proteins termed the pericentriolar material (PCM). The more mature mother centriole, which has subdistal and distal appendages, is connected to the daughter centriole by a proteinaceous material named the linker. (B) Electron micrograph of the centrosome. The top inset indicates a cross-section of subdistal appendages; the bottom inset indicates a cross-section of the proximal part of the centriole. Note the triplet microtubules (MTs) Scale bar: 0.2  $\mu\text{m}$ . (Adapted from Bettencourt-Dias, et al., 2007).

The two centrioles are barrel-shaped, nine triplets MTs structures, about 0.2  $\mu\text{m}$  in diameter and approximately 0.3 to 0.5  $\mu\text{m}$  in length<sup>30</sup>. The more mature centriole – mother centriole - has subdistal and distal appendages, whereas the immature centriole does not – daughter centriole. Centrioles, which are linked by a proteinaceous material named the linker, are critical for recruiting the surrounding PCM to anchor and nucleate MTs<sup>30,34,41</sup>(Figure 1.2).

Centrioles are polarized along the proximo–distal axis<sup>30</sup>, and at the distal end of the mother centriole have specialized structures known as appendages. The appendages have important structural roles in cilia formation, cell polarity, and microtubule organization, which are critical for maintaining cellular integrity and function<sup>30</sup>. The distal appendages typically anchor the centriole to the plasma membrane during ciliogenesis, while the subdistal appendages may play roles in MT organization and anchoring. The PCM is fibrillar material composed of hundreds of proteins, including those responsible for centriole assembly, duplication, elongation, and maturation, and those implicated in MT nucleation, such as pericentrin,  $\gamma$ -tubulin rings, motor proteins, and regulatory molecules<sup>30,39,41</sup>.

Over the past two decades, our understanding of centrosome functions has greatly expanded<sup>34</sup>. Below, the primary functions of centrosomes are outlined, illustrating their critical roles in cellular biology (Table 1.1).

**Table 1.1 - Centrosomes Functions.**

Function	Description
<b>Microtubule Organization</b>	Centrosomes nucleate and anchor MTs, determining their spatial arrangement within the cell. This is crucial for maintaining cell shape, polarity, and intracellular transport <sup>30,34</sup> .
<b>Spindle Formation During Mitosis</b>	Pivotal in mitotic spindle assembly and essential for chromosome segregation during cell division. Centrosomes ensure the proper attachment of microtubules to chromosomes and contribute to separating sister chromatids during anaphase <sup>42</sup> .
<b>Regulation of Cell Cycle Progression</b>	Proper centrosome duplication is tightly regulated during the cell cycle. Centrosomes help coordinate G1/S transition, DNA replication, and the initiation of mitosis <sup>40</sup> .
<b>Ciliary Function</b>	In non-dividing cells, the centrosome can form a basal body, which acts as a template for forming cilia and flagella. This is essential for cellular motility and sensory functions like signaling pathways involved in development and tissue homeostasis <sup>30</sup> .

<b>Cell Polarity and Migration</b>	Positioning microtubules contributes to establishing cell polarity, which orients cellular structures and organelles. This organization is crucial for cell migration, tissue development, and wound healing <sup>30</sup> .
<b>Role in Cytokinesis</b>	Centrosomes assist in organizing the actin-myosin contractile ring during cytokinesis (the final separation of daughter cells after mitosis), ensuring accurate cell division and proper inheritance of cellular components <sup>30,40</sup> .
<b>Signaling Hub</b>	Emerging research indicates centrosomes may act as a signaling platform, influencing key processes such as DNA damage repair, stress responses, and cell cycle checkpoints <sup>30,34,43</sup> .
<b>Maintenance of Genomic Stability</b>	Centrosomes coordinate accurate chromosome segregation and regulate cell division. They also help prevent aneuploidy and other forms of genomic instability that can lead to cancer development <sup>30,44</sup> .

### 1.2.2 The centrosome duplication cycle

Each time cell division occurs, centrosomes and DNA are duplicated. These are semiconservative processed and occur only once per cell cycle: centrioles are duplicated once, like DNA, ensuring that each daughter cell inherits one centrosome (with two centrioles)<sup>30,39,40</sup>.

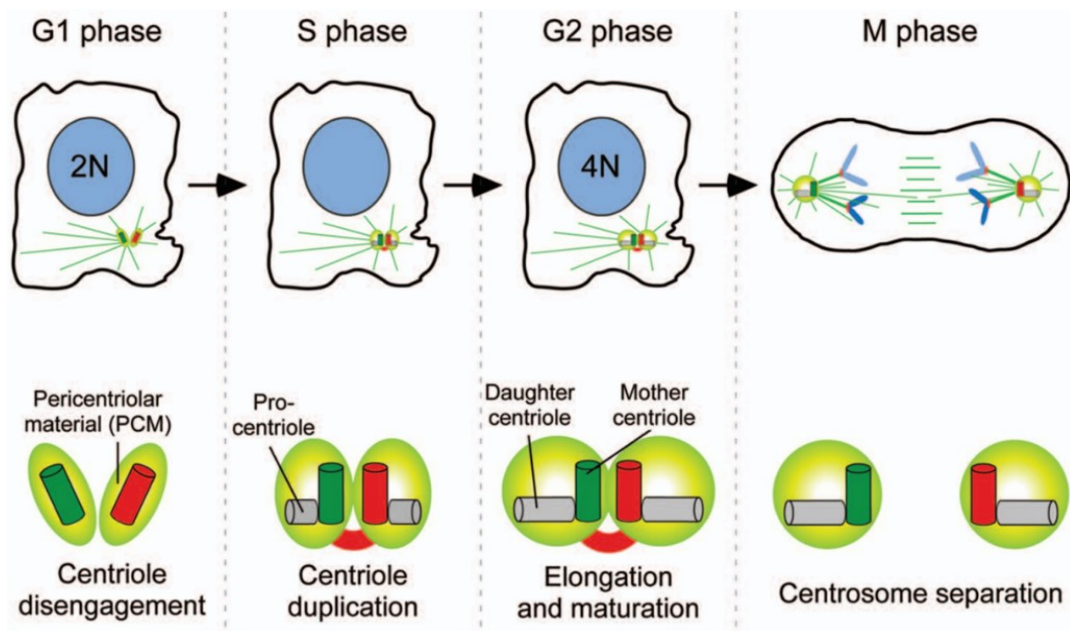


**Figure 1.3 - The centrosome duplication cycle.** The duplication is tightly regulated and synchronized within the cell cycle. It comprises four stages: centriole disengagement, duplication, elongation/maturation, and separation. Each centriole duplicates only once per cell cycle, and only one centriole is formed next to a pre-existing one. (Adapted from Holland et al.,2010).

Centrosome duplication occurs in four consecutive stages: 1) disengagement of the centrioles at the end of mitosis, 2) nucleation of the daughter centrioles (also known as procentrioles before they acquire full centriolar length) in G1/S, 3) elongation of the procentrioles (S and G2), and 4) separation of the centrosomes (G2–M)<sup>30,38,40,41</sup> (Figure 1.3). At the end of mitosis, the new mother centriole acquires the appendages (centriole maturation) crucial in cilia formation and intracellular signaling<sup>40,45</sup>. In humans, intricate regulatory mechanisms control the timing and location of centriole duplication, ensuring that it occurs accurately and only once per cell cycle<sup>46</sup>. PLK4 and SAS6 are two proteins that cooperate for centriole duplication<sup>47</sup>. Polo-like kinase 4 (PLK4) is the primary regulator of centrosome duplication. Its kinase activity is essential for initiating centriole duplication. It phosphorylates various substrates, including STIL, to facilitate the recruitment of other proteins necessary for centriole formation and promote downstream events necessary for centriole assembly<sup>47</sup>. Excess PLK4 activity leads to extra centrioles, and its depletion causes decreased centriole numbers<sup>48</sup>. PLK4 activity is regulated mainly through SCFbTrCP/ubiquitin-dependent proteolysis and autophosphorylation. As the ubiquitin-proteasome system rapidly degrades PLK4, this regulatory mechanism prevents excessive centriole formation and makes PLK4 relatively scarce and transient within the cell<sup>40,46</sup>.

Another important core protein is SAS6, whose levels are also controlled by proteolysis<sup>47</sup>. SAS6 co-localizes with STIL and PLK4 during interphase at the two newly formed procentrioles. SAS6 is a key structural component that assembles into a cartwheel-like structure at the centriole. This structure serves as a scaffold that ensures the assembly of MTs in a ninefold symmetry that is essential for the formation of new centrioles<sup>30,40,46</sup>.

After initial formation, procentrioles are stabilized and elongated until the G2 phase, which involves CPAP/SAS-4<sup>38</sup>. CP110 and Cep97 act like "caps" at the ends of centrioles, controlling their length to ensure they don't grow too long<sup>30,38,39</sup>. They associate with the distal ends of the centrioles and likely function as capping proteins. During centrosome maturation, in G2/M phases, there is an increased accumulation of PCM, driven by Plk1 and Aurora A kinases<sup>40</sup>. At that stage, the dissolution of the protein linker between the two original parental centrioles allows the separation and migration of the two centrosomes to opposite poles of the cell to organize the bipolar mitotic spindle. At the end of the M phase, centriole disengagement, through the activities of PLK1 and Separase, prepares the centrioles for duplication in the following S phase<sup>38</sup>.

The centrosome duplication cycle is of major importance in correct cell division<sup>40,46,49</sup>. If not properly coordinated, cells may acquire centrosome anomalies that affect cell homeostasis.

### **1.3 Centrosome Deregulation and Cancer**

Centrosome anomalies have been largely subdivided into two main categories: structural and numerical. Although conceptually different, they usually occur together in tumors<sup>38</sup>. Structural deviations are anomalies in the centriole shape and/or in the amount, composition, or even phosphorylation state of PCM components. The accumulation or loss of a centrosome causes numerical alterations. Extra centrosomes, or centrosome amplification (CA), is the most frequent defect detected in human cancer<sup>35,36</sup> and has also been detected in cancer-associated human diseases<sup>50–52</sup>.

CA has been linked to cancer initiation and progression<sup>27,50,53</sup>. Experimental models show that CA can drive tumor formation, and clinical studies indicate that CA levels correlate with tumor stage and invasiveness across various cancers<sup>50,54–57</sup>. Findings of CA in the late stages of cancer are very frequent, which substantiates the involvement of extra centrosomes in cancer progression and metastasis<sup>27,52,56</sup>. Furthermore, concerning the degree of differentiation, these abnormalities tend to be more pronounced in high-grade neoplasia (aggressive and poorly differentiated) than in low-grade neoplasia (more differentiated, less aggressive tumors)<sup>54,56,58,59</sup>. CA is also linked to some other clinical criteria of aggressiveness and, therefore, poor prognosis, such as lymph node and/or distant metastasis, early recurrence of tumors, and poor survival<sup>52,59–62</sup>. Overall, the evidence supports a key role for CA in carcinogenesis.

#### **1.3.1 Causes and consequences of centrosome amplification**

Studies in cultured cells<sup>29,58</sup> and animal models<sup>53</sup> have shown that CA may ensue from cytokinesis failure, mitotic slippage, cell-cell fusion, overduplication of centrioles, and de novo centriole assembly<sup>54</sup>.

CA has devastating consequences on cell homeostasis (Figure 1.4). During cell division in normal cells, CA normally results in impaired cell cycle progression<sup>63</sup> and/or programmed cell death (apoptosis) to prevent the propagation of potentially harmful

mutations and maintain tissue homeostasis<sup>38</sup>. However, acquired oncogenic mutations or loss of tumor suppressor genes (such as *TP53*)<sup>46</sup> may favor cells with CA to survive and proliferate. Moreover, cancer cells can also overcome the inhibitory effect of extra centrosomes<sup>64</sup>, by developing mechanisms to deal with CA during cell division, which allows them to continue dividing successfully<sup>36</sup>. A major coping mechanism known is centrosome clustering: cells cluster their extra centrosomes so that cells can undergo pseudo-bipolar mitosis<sup>37,38</sup>. However, the erroneous attachment of chromosomes to the mitotic spindle during cell division (merotelic attachment) still impacts chromosome segregation<sup>46</sup>. Other CA coping mechanisms, like centrosome extrusion and inactivation of extra centrosomes, allow maintenance of functional mitotic spindles, regulation of the spindle assembly checkpoint, extending the duration of some phases in the cell cycle to allow additional time to resolve issues related to centrosome function and chromosome alignment<sup>38</sup>.

CA can, therefore, contribute to chromosomal instability (CIN)<sup>61,65</sup> and aneuploidy. Nevertheless, the role of extra centrosomes is not limited to mitosis. Indeed, recent

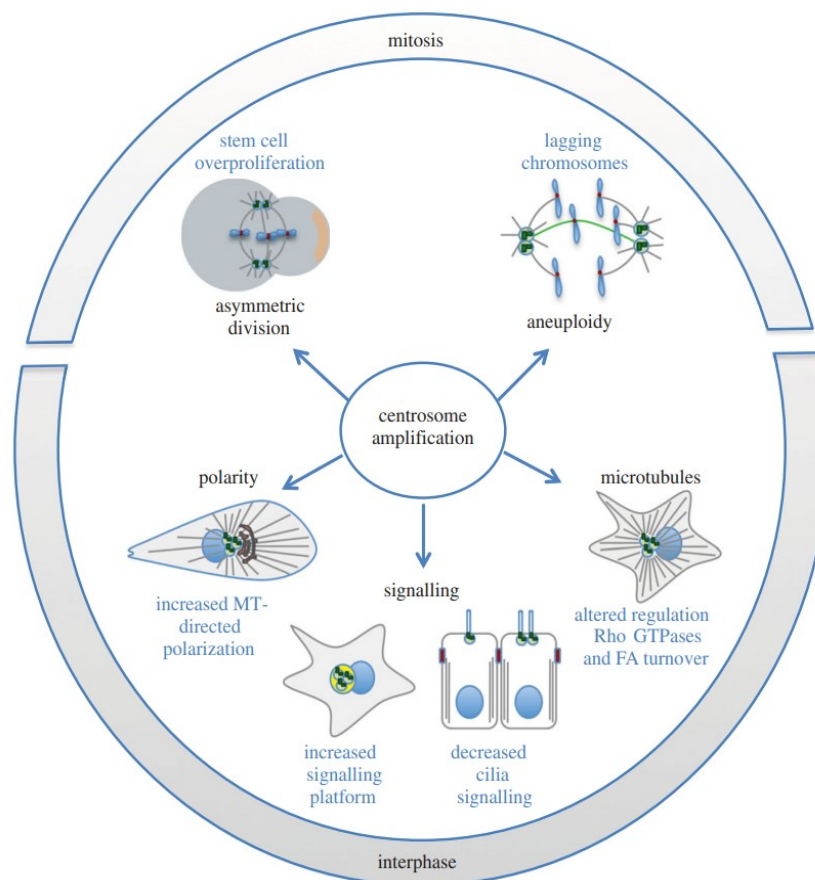


**Figure 1.4 - Consequences of centrosome amplification in cancer.** In mitosis, CA promotes CIN, chromosome missegregation and impairs asymmetric cell division. In interphase, CA can affect the migration and invasive properties of cells, as well as polarity and signaling (Adapted from Godinho, S. A. & Pellman, D., 2014).

studies have shown that CA also contributes to i) defective ciliary signaling, ii) disrupted cell polarity and tissue architecture<sup>36</sup>; iii) invasive behavior<sup>66</sup>, iv) increased metastatic potential<sup>55,62,67</sup>; and v) therapeutic resistance<sup>38,63</sup>.(Figure 1.4).

### 1.3.2 Centrosome amplification and cell invasion

Cell invasion is a hallmark of cancer<sup>38</sup>. Notably, several pieces of evidence for CA are associated with migration and invasion<sup>54,56,68</sup>.

One of the first experimental pieces of evidence came from a study showing that CA can induce invasive protrusions in 3D cultures of mammary epithelial cells through i) activation of Rac1, a small GTPase that regulates actin dynamics and that leads to the formation of protrusions that help cells migrate; ii) increase in MTs nucleation and the subsequent changes in cell shape and motility, facilitating the movement of cancer cells into adjacent tissues<sup>54</sup> (Figure 1.5). Another experimental piece of evidence came from a study showing that PLK4 influences cell motility and ECM interactions through the activation of RAC1-Arp2/3 signaling pathway<sup>55</sup> (Figure 1.5). This pathway is instrumental in regulating actin dynamics, which are critical for cellular movement and the interactions between cells and the ECM.

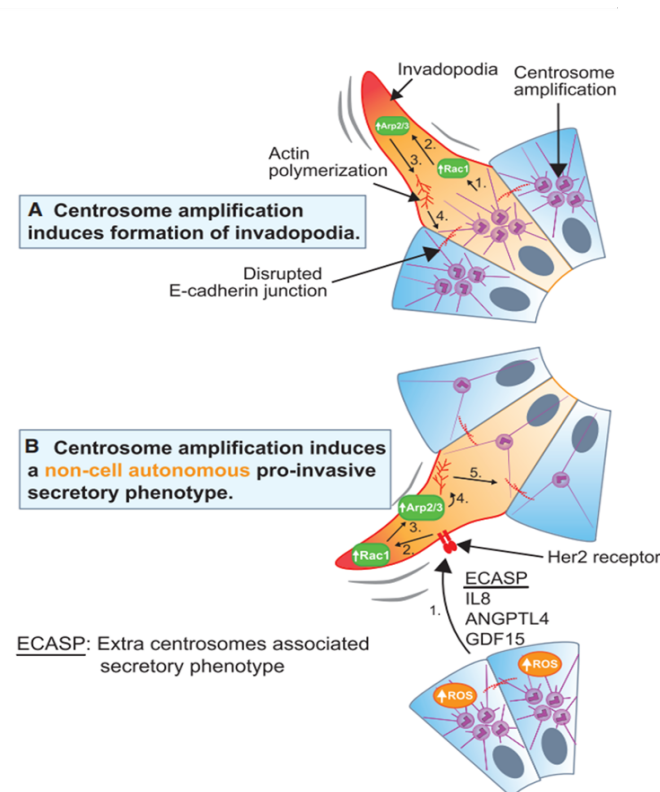


**Figure 1.5 - CA can promote invasive phenotypes.** Centrosome amplification can induce the formation of invadopodia and a non-cell autonomous pro-invasive secretory phenotype. (Adapted from LoMastro and Holland, 2019).

A recent study in cultured mammary MCF10A cells and in *in vivo* model using chick embryo xenografts showed increased Rac1 activity upon CA, promoted invasion by disrupting cell-cell junctions, enhancing cell-ECM attachment, activating MMPs, and engaging small GTPase signaling pathways, all of which contribute to a more aggressive and invasive cancer phenotype<sup>57</sup>.

Extra centrosomes have also been reported to form reactive oxygen species (ROS), promoting oxidative stress in cells<sup>66</sup>. This drives the release of an extra-centrosomes associated secretory phenotype (ECASP) composed of pro-invasive factors (e.g. IL-8, ANGPTL4, and GDF-15). In turn, the secreted pro-invasive factors activate signaling pathways in adjacent cells. This study demonstrates that CA can affect the behavior of neighboring cells through a non-cell-autonomous mechanism, that influences cells without centrosome defects to exhibit invasive behaviors in response to the factors secreted by the aberrant cells, contributing to an expanded invasive tumor phenotype<sup>66</sup> (Figure 1.5). Another recent study in pancreatic ductal adenocarcinoma cells reported that CA could indirectly lead to invasion by promoting the secretion of exosomes, vesicles generated through the fusion of the multivesicular bodies with the plasma membrane<sup>67</sup>. Hence, extra centrosomes may also promote invasion by altering signaling pathways, changing the cell cargo secreted to the extracellular matrix (ECM) either by an extra centrosome-associated secretory phenotype (ECASP) of several cytokines and chemokines or by small extracellular vesicles<sup>67</sup>.

So, CA appears to be closely associated with changes in the cytoskeleton and signaling pathways that augment cancer cells' ability to remodel the ECM, facilitating more effective migration and invasion through tissues.

#### **1.4 Centrosome amplification and Barrett's Esophagus tumorigenesis**

BE progression to EAC is characterized by a high mutation rate and the accumulation of CIN and aneuploidy<sup>6,16</sup>, common outcomes of centrosome amplification<sup>37,69</sup>. Although important, many studies about BE tumorigenesis have focused solely on gene alterations<sup>70,71</sup>, overlooking how alterations in cellular structures, such as the centrosome, contribute to the rise of carcinogenic pathways.

Our research group has focused on the influence of CA on the progression of carcinogenic pathways from BE to EAC. Employing the BE cancer model, we have contributed to the growing body of knowledge about the stages at which CA emerges and explores its role in malignant transformation and progression. Indeed, our work has revealed that CA arises early in metaplasia and was only detected in metaplasia samples of BE patients that progressed to neoplasia and never in metaplasia samples

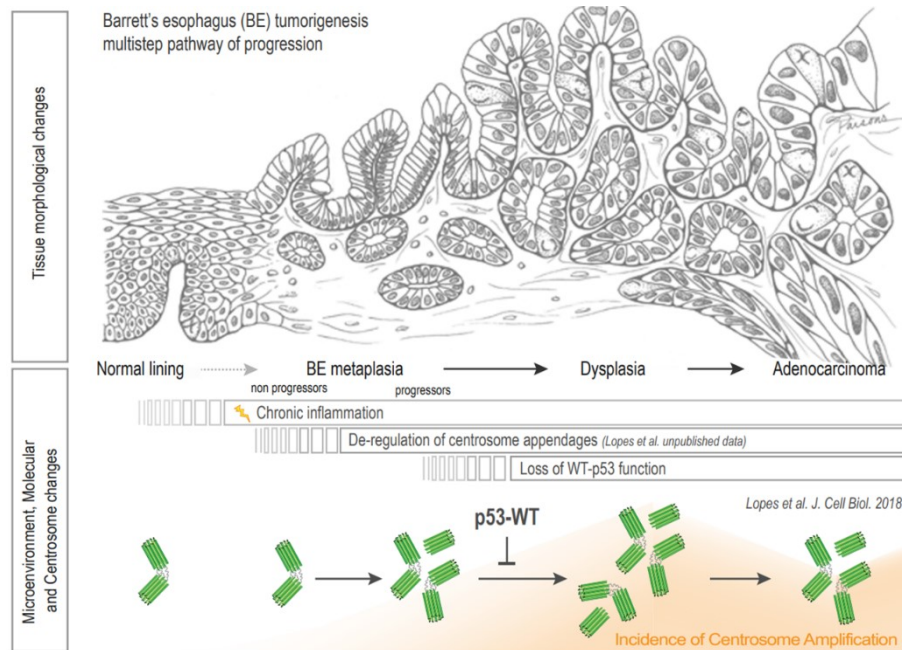


**Figure 1.6 - Barrett's Esophagus progression and centrosome amplification.** Schematic representation of the presence and incidence of CA at the different stages of BE malignant transformation and progression. (Adapted from Lopes et al, 2018.)

of non-progressed patients<sup>27</sup>.

Moreover, we found that CA was detected in all subsequent steps of progression and that its incidence significantly increased from metaplasia to dysplasia<sup>27</sup>. Together, these findings show that CA is a frequent feature in BE progression and may contribute to tumor initiation and progression. Particularly, seeing that the incidence of CA was most prominent in dysplasia cells, which have been shown to exhibit an increased migratory and invasive potential<sup>29</sup>, and that CA has been shown to induce invasion in mammary cells<sup>54,72</sup> our observations strongly suggested that CA may contribute to BE progression by promoting invasion of dysplasia (Figure 1.6). Preliminary studies in our laboratory explored two methods to reduce CA levels in dysplasia cells of the BE

model. With this, we aimed to test if such a reduction in CA levels could reduce cell invasion and migration. Using 3D cultures, such as those used in previous studies of CA impact on invasion in mammary cells<sup>54</sup>, our preliminary work suggested that reducing CA levels could indeed reduce the invasion capacity of dysplasia cells. Interestingly, the reduction of CA levels was accompanied by changes in the levels of epithelial marker E-cadherin and the mesenchymal markers vimentin and fibronectin. These observations suggest that changes in the invasiveness potential in dysplasia cells resulting from reduced CA levels could be due to alterations in the epithelial-mesenchymal transition (EMT) state. However, further studies are needed to test the contribution of CA in the migratory and invasiveness capacity of dysplasia cells.

## **1.5 Centrosome amplification, EMT changes, and BE progression**

Epithelial-mesenchymal transition (EMT) is a naturally occurring process in embryonic development and wound healing<sup>73</sup>. However, cancer cells can also use this process to promote cancer cell invasion and metastasis<sup>74,75</sup>. The EMT and the reverse process mesenchymal-epithelial transition (MET) also play important roles in stem cell differentiation and de-differentiation (or reprogramming)<sup>75</sup>.

EMT is when epithelial cells lose their epithelial characteristics and acquire mesenchymal characteristics, structure, and biological function<sup>73</sup>. During cancer invasion through EMT, epithelial cells transform into a mesenchymal state by down-regulating epithelial markers such as E-cadherin and up-regulating mesenchymal genes such as fibronectin and vimentin<sup>75</sup>, and matrix metalloproteinases (MMPs)<sup>57</sup>. Overall, this transformation allows primary epithelial tumor cells to disseminate from the original site and migrate into the surrounding stroma<sup>29,74</sup>. Interestingly, cells with decreased levels of E-cadherin and CA are able to cluster their extra centrosomes and survive, showing an increased tolerance for cells with CA, just like cancer cells<sup>64,76</sup>. Moreover, recent data suggest that upregulation of PLK4 can induce EMT through Wnt/ $\beta$ -catenin signaling in colorectal cancer, where PLK4 overexpression is associated with enhanced tumor size, lymph node metastasis, and EMT alterations<sup>77</sup>. However, there is no clear evidence that CA itself leads to EMT.

The BE model has few studies that investigate EMT. In particular, one study showed that non-neoplastic BE metaplasia cells exposed chronically to acid and bile salts undergo malignant transformation and develop EMT<sup>29</sup>. However, it is unclear if EMT is

induced directly by exposure to acid or bile salts or the result of subsequent malignant transformation and if EMT is acquired through a compilation of other mutagenic factors<sup>29</sup>.

### 1.5.1 Vimentin and Fibronectin

Mesenchymal markers like vimentin and fibronectin appear to be augmented at the onset of invasiveness.

**Vimentin** is a type III intermediate filament with tubulin-based microtubules and actin-based microfilaments constituting the cytoskeleton that plays a major role in supporting and anchoring the position of organelles in the cytosol<sup>78</sup>. It is universally expressed in normal mesenchymal cells and is regarded as a canonical marker of EMT<sup>79</sup>. Vimentin plays a significant role in cancer progression due to its involvement in various tumorigenic processes. Vimentin overexpression is often reported in cancer cell lines of the lung, prostate, and breast<sup>78</sup>. In gastrointestinal tumors with patient-derived tumor samples, vimentin overexpression was associated with aggressive tumor behavior, increased invasion, and poor prognosis for patients<sup>80</sup>. Though its expression is best characterized in the EMT process, it is equally possible that tumor cell migration and invasion are a consequence of vimentin overexpression in cancer cells, as most studies have indicated a positive association between the invasive phenotype and vimentin overexpression and have shown a decrease in these characteristics upon knockdown of vimentin in vitro<sup>81–83</sup>. Finally, vimentin may act as a scaffolding protein during signal transduction, interacting with various oncogenes by being part of the downstream effects of oncogenic signaling pathways (e.g., TGF- $\beta$ , PI3K/Akt, Wnt/ $\beta$ -catenin, NF- $\kappa$ B, and Rho GTPase pathways<sup>80</sup>), transcription factors (e.g., TWIST, ZEB, SNAIL<sup>29,84</sup>), and receptor tyrosine kinases (e.g., EGFR), which collectively promote tumorigenic events.

**Fibronectin** is a high-molecular-weight adhesive glycoprotein in the extra-cellular matrix (ECM). It is highly expressed in embryonic tissues, wound healing, inflammation, and various tumors, suggesting a role in tissue remodeling<sup>85</sup>. Initially, it was identified as a cell surface glycoprotein present on the surfaces of non-transformed cell lines. Fibronectin mRNAs, approximately 8-kb in size, encode for fibronectin protein subunits, which vary in size from 230–270 kDa due to alternative splicing<sup>86</sup>. Fibronectin functions serve various critical roles in cellular interactions with the ECM: i) cell adhesion: serves as a substrate for cell attachment, facilitating the binding of cells to the ECM; ii) cell migration: provides a pathway for cells to move through the ECM; iii) cell growth and differentiation by interacting with various growth factors and can modulate their activity;

iv) matrix assembly, it plays a role in the assembly of the matrix itself and self-associates to form fibrils, which are essential for the structural organization of the ECM; v) fibronectin binds to other molecules through multiple binding sites for other ECM components, such as collagen and fibrin, which are essential for tissue repair and remodeling. It also binds to glycosaminoglycans, which can influence cell adhesion and migration<sup>87</sup>. Fibronectin has conflicting roles in cancer<sup>88</sup>. As a result, before considering fibronectin as a target for cancer therapy, the actual role of fibronectin in a given context must be known.

When cancerous fibronectin is expressed early, it is known to have a tumor-suppressing role, helping to prevent tumor transformation and halting early tumor progression<sup>88</sup>. In the late stages of cancer, fibronectin can also promote metastasis, for instance, by promoting the formation of a premetastatic niche and by correlating to a poor prognosis<sup>89,90</sup>. Moreover, the fibronectin matrix, deposited in tumor microenvironments (TMEs), influences this environment by promoting early tumor progression<sup>88</sup>. Interestingly, the presence of fibronectin in TMEs is paradoxically correlated with better prognostic outcomes acting as an oncogenic factor in the surrounding stromal tissues<sup>88,89</sup>.

In the esophagus, a study showed that fibronectin is upregulated in adenocarcinoma samples<sup>29</sup> being a part of an EMT signature. At the same time, its expression in normal mucosa, metaplasia, and dysplasia is more or less similar<sup>85</sup>. In esophageal squamous cell carcinoma (ESCC), fibronectin expression and secretion in ESCC cell lines were found to be low, but these cells adopted a more migratory phenotype when cultured *in vitro* in a microenvironment containing high levels of fibronectin<sup>91</sup>.

Interestingly, fibronectin secretion is crucial in maintaining cancer cells' invasive potential. Impairment in fibronectin secretion disrupts cell-ECM interactions, impairs cell motility, and alters signaling pathways associated with invasion, ultimately reducing metastatic capabilities<sup>92</sup>. In the context of ovarian cancer, mesothelial cells secrete more fibronectin, which has been linked to increased adhesion, invasion, and proliferation of tumoral cells<sup>93</sup>. This phenomenon was tested in 3D organotypic 3D cultures, conditioned media from mesothelial cell experiments, and *in vitro* and murine models. In a prostate cell cancer model, findings reveal that an inhibitor of Hsp90 significantly impacts cell motility and invasion by dysregulating fibronectin trafficking<sup>92</sup>. This substance disrupts the normal trafficking and secretion of fibronectin, which could contribute to its anti-invasive effects in prostate cancer cells.

Fibronectin deposition in the ECM is also by itself another cancer-promoting event<sup>86</sup>. Fibronectin promotes cell motility by activating signaling pathways that induce cytoskeletal reorganization<sup>88</sup>. A fibronectin-rich ECM is a scaffold that cancer cells can adhere to and migrate through, facilitating their invasion into adjacent tissues and contributing to metastasis. Moreover, fibronectin interacts with MMPs, enzymes that degrade the ECM<sup>91,94,95</sup>.

## 1.6 Aims and Objectives

Barrett's Esophagus (BE) has a relatively low incidence rate, but its progression to esophageal adenocarcinoma (EAC) results in cancer with high morbidity and mortality, particularly if not diagnosed early<sup>4,25</sup>. The diagnosis of BE and the pathological assessment of dysplasia are critical for clinical decision-making<sup>8</sup>. Despite the utility of biopsy in detecting dysplasia, it has notable limitations. Therefore, understanding the mechanisms that trigger the transformation of metaplastic cells into dysplastic cells is essential for identifying potential biomarkers for early diagnosis and intervention.

One key feature of BE progression is the increase in the incidence of centrosome amplification (CA)<sup>27</sup>, which has been reported to contribute to the development of oncogenic characteristics such as cellular invasion<sup>54,62</sup>. With this work, I aimed to investigate the impact of CA in promoting migration and invasion in the context of BE progression. The specific objectives of this research were to:

1. Test if CA reduction alone is sufficient to reduce the migratory and invasive potential of BE dysplasia cells.
2. Identify the molecular mechanisms by which CA contributes to the migratory and invasiveness capacity of BE dysplasia cells.

In this study, we aim to advance the field of cancer research by elucidating the molecular pathways through which CA influences the progression of Barrett's esophagus (BE). Our findings are intended to enhance the current understanding of centrosomes, thereby expanding the repertoire of potential biomarkers that could inform and optimize personalized treatment strategies for BE, ultimately improving patient outcomes.

## 2. Material and Methods

### 2.1 Cell culture

#### 2.1.1 Cell line maintenance

Cell lines hTERT CP-D cell lines obtained from biopsies of patients with high-grade dysplasia (from P. Rabinovitch, Univ. of Washington, Seattle)<sup>96</sup> were maintained in MCDB 153 medium (Sigma) supplemented with 5% Fetal Bovine Serum (Sigma), 4 mM L-Glutamine (Thermo Fisher Scientific), 0.1% Insulin transferrin-sodium-selenite (Sigma), 100 U/ml penicillin-streptomycin (Thermo Fisher Scientific), 140 µg/ml Bovine Pituitary Extract (Thermo Fisher), 20 µg/ml adenine (Sigma), 0.4 µg/ml hydrocortisone (Sigma), 1 nM cholera toxin (Sigma) and 20 ng/ml Epidermal Growth Factor (Sigma)<sup>96</sup>. Cells were maintained at 37°C in humidified air with 5% CO<sub>2</sub>. To passage or collect cells, cells grown to confluence in monolayer were detached: after removing growing media, cells were incubated with Tryple (Thermo Fisher Scientific) for 3-5 minutes at 37°C to detach cells; cells were then resuspended using full media.

#### 2.1.2 siRNA transfection

Cells were seeded at densities of either 5 x 10<sup>4</sup> cells/well on glass-coverslips in 24-well plates or 10 x 10<sup>4</sup> cells/well in 6-well plates. After 24 hours of adhesion, endogenous *PLK4* (5'-GGTGAAAATACATTGCCAATT-3'), *SAS6* (5'-GCACGTTAATCAGCTACAA-3'), or *FN1* (5'-GAAUAGAUGCAACGAUCA-3') were depleted using specific siRNA oligonucleotides (Dharmacon). Control cells were either mock-treated or transfected with luciferase siRNA (*GL2*; 5'-CGTACGCGGAATACTTCGA-3'; Dharmacon). Cells were transfected with 50 nM siRNA oligonucleotides using Lipofectamine RNAiMAX (Thermo Fisher Scientific), per the manufacturer's protocol. After depletion (for specific time points, see Figure 3.1A), cells seeded on coverslips in 24-well plates were fixed using either (i) ice-cold methanol for 10 minutes at -20°C; (ii) or 4% paraformaldehyde for 10 minutes at room temperature (RT). Cells seeded on 6-well plates cells were collected for (i) cell viability assessment, (ii) Western blotting, (iii) mRNA depletion analysis by Real-Time Quantitative Reverse Transcription (RT-qPCR), (iv) transwell Boyden migration and invasion assays, or treated to collect condition media to detect protein secretion using an enzyme-linked immunosorbent assay (ELISA).

### **2.1.3 Cell Viability Assessment**

The Trypan Blue Exclusion Test was used to evaluate the impact of *PLK4*, *SAS6*, or *FN1* depletion on cell viability. Transfected cells were detached from 6-well plates as described above (2.1.1). 10  $\mu$ l trypan blue dye were added to 10  $\mu$ l of resuspended cells. After three minutes of incubation, 10  $\mu$ l were loaded onto a hemacytometer. Viable cells excluded the dye, while non-viable cells absorbed it. The percentage of viable cells was then calculated.

### **2.1.4 Transwell migration and invasion assays**

Following a 72-hour transfection period, cells seeded on a 6-well plate were serum-deprived for 4 hours and then detached (2.1.1) and resuspended in the same medium. Subsequently,  $4 \times 10^4$  cells were seeded onto the upper compartment of transwell inserts in 24-well plates. Inserts with standardized Matrigel-coated membranes were utilized for invasion assays, while inserts without Matrigel-coated membranes were used for migration tests. The lower chamber of the transwell system was filled with a chemoattractant standard full-growth media. The cells were then incubated at 37°C with 5% CO<sub>2</sub> for 22 hours. After incubation, non-invaded and non-migrated cells remaining in the upper chamber were removed using a cotton swab. The cells on the underside of the membrane were fixed then with ice-cold methanol for 10 minutes at -20°C. After three washes with 1X PBS cells were incubated with Hoechst 33342 to stain DNA, washed again, and finally mounted on glass slides with Vectashield. Cell counting was performed in approximately five randomly selected fields using a fluorescence microscope with a 10x objective lens.

## **2.2 RT-qPCR**

Transfected cells were detached from 6-well plates as described above (2.1.1). Resuspended cells were centrifuged for 3 minutes at 1,100 rpm. After removal of the supernatant, cell pellets were snap-frozen in liquid nitrogen and stored at -80°C until use. Cell pellets were then used to extract RNA using the Qiagen RNeasy kit following the manufacturer's protocol. For cDNA synthesis, 1  $\mu$ g of RNA was reverse transcribed using the High-Capacity RNA-to-cDNA™ Kit (Thermo Fisher Scientific), following the manufacturer's instructions. Quantitative real-time PCR (RT q-PCR) was carried out

using Power SYBR Green, and the reactions were analyzed on an ABI QuantStudio 7 Flex Real-Time PCR System (Applied Biosystems). All primers used for RT q-PCR are listed in **Table 2**.

**Table 2.1 - Primer sequences used in the RT-qPCR.**

GENE SYMBOL	FORWARD PRIMER 5'-3'	REVERSE PRIMER 5'-3'
<i>PLK4</i>	AGACCACCCCTTCGACACTGA	GTCCTTGGCCTCTATTGACAAA
<i>SAS6</i>	GAATGGGCGTCACATACAGC	TTGATATTGAACCTGTGCCTGC
<i>FN1</i>	AACTGCAAACCTCCGTCACCC	GAGGGCACTGTATCTGAGCG
<i>E-CADHERIN</i>	GAGGGGTAAAGCACAAACAGC	TGACCCTTGACGTGGTGG
<i>VIMENTIN</i>	CAGCTAACCAACGACAAAGCC	CTCCTCCTGCAATTTCTCCCG
<i>GAPDH</i>	ACATCGCTCAGACACCATG	TGTAGTTGAGGTCAATGAAGGG

## 2.3 Western Blot

### 2.3.1 Cell lysis, SDS-PAGE and transfer

Transfected cells were detached from 6-well plates as described above (2.1.1). Resuspended cells were centrifuged for 3 minutes at 1,100 rpm. After removal of the supernatant, cell pellets were snap-frozen in liquid nitrogen and stored at -80°C until use. Cell lysates were generated by resuspending the pellets in a lysis buffer containing 50 mM Hepes (pH 7.4), 100 mM KCl, 1 mM EGTA, 1 mM MgCl<sub>2</sub>, 10% glycerol, 0.05% NP-40, a 1× protease inhibitor cocktail, and 1× phosphatase inhibitors. The resuspension was incubated on ice for 20 minutes. The lysates were then centrifuged at 14,000 rpm for 10 minutes at 4°C. Protein concentration in the resulting supernatant was measured using the Bradford assay (Bio-Rad). 60 µg of protein was mixed with Laemmli buffer, boiled at 95°C for 5 minutes, and subsequently loaded onto pre-cast 4-12% gradient polyacrylamide gels (Invitrogen). The proteins were transferred onto nitrocellulose membranes using a semi-dry transfer method at 20 V for 1 hour. Blocking was performed for 1 hour at room temperature in TBS containing 5% milk powder. Primary antibodies were incubated overnight at 4°C, followed by secondary antibody incubation on the following day for 1 hour at room temperature,

both in TBST (0.1% Tween-20 [Sigma] in TBS) supplemented with 1% milk powder. After each antibody incubation, the membranes were washed with TBST.

### **2.3.2 Protein detection**

Primary antibodies used for western blotting were against fibronectin (1:500; mouse; Santa Cruz Biotechnology), SAS6 (1:200; mouse; Santa Cruz Biotechnology), E-cadherin (1:1000; rabbit; Santa Cruz Biotechnology), vimentin (1:200; mouse; Santa Cruz Biotechnology) and GAPDH (1:1000; rabbit; Cell Signalling). The secondary antibodies used IRdye 680CW (1:10000; rabbit; Li-COR) and IRdye 800CW (1:10000; mouse or rabbit; Li-COR) and membranes were developed and quantified on the Odyssey Scanner (Li-COR).

## **2.4 Immunofluorescence microscopy**

### **2.4.1 Cell fixation**

For centrosome staining, cells grown on coverslips were fixed and permeabilized with ice-cold methanol at -20°C for 10 minutes (min) in the 24-well plates. Cells were then washed three times (5 minutes each) with 1X Dulbecco's Phosphate Buffered Saline (PBS; Biowest) before being processed as below (2.4.2).

For EMT markers, cells grown on coverslips were fixed with paraformaldehyde (PFA) for 10 minutes (min) at RT in the 24-well plates. After 3 washes with PBS, cells were then permeabilized with 0.1% Triton solution for 10 minutes at RT. Cells were then washed 3 times with PBS before being processed as below (2.4.2).

### **2.4.2 Immunofluorescent staining**

Cells were blocked with Blocking Solution (see below) for 30 minutes at RT. Primary antibodies were diluted in Blocking Solution and applied to the cells on coverslips, followed by incubation overnight at 4°C in a humidified chamber. The following day, cells were washed three times with PBS. Secondary antibodies, also diluted in the Blocking Solution, were then added to the cells and incubated for 1 hour at room temperature in the dark. After three additional washes with PBS, cells were stained with 1 µg/ml Hoechst 33342 in PBS for 10 minutes. Following this, cells underwent a final wash, and the coverslips were mounted onto glass slides using VECTASHIELD

Mounting Medium (Vector). The slides were stored in a slide holder at 4°C. Blocking Solutions: (A) 10% FBS in PBS for centrosome staining; (B) 3% bovine serum albumin (BSA) for EMT markers staining.

### **2.4.3 Antibodies**

For centrosome staining, primary antibodies targeting pericentrin (1:5000, rabbit, Abcam, ab4448) and centrin (clone 20H5; 1:500, mouse, Millipore, 04-1624) were used. For detecting EMT markers, primary antibodies against E-cadherin (1:1000, rabbit; Cell Signaling), vimentin (1:1000, mouse; Santa Cruz), and FN1 (1:100, mouse; BD Biosciences) were used. Secondary antibodies used were Rhodamine Red (1:500, rabbit, Jackson ImmunoResearch Laboratories, Inc.) and Alexa Fluor 488 (1:500, mouse, Thermo Fisher Scientific).

### **2.4.4 Image Analysis**

Immunofluorescence microscopy images were captured at room temperature using an inverted Zeiss Axio Observer 7 SP Confocal microscope with a Plan Apochromat 63x 1.40 NA oil objective and Zen black software. The images were captured as a z series with a 0.2 (centrosome staining) or 0.4 (EMT markers)  $\mu\text{m}$  z interval and are displayed as maximum-intensity projections prepared using Image J software (National Institutes of Health).

### **2.4.5 Centriole Count**

Centrioles were identified and quantified based on the colocalization of the centriole marker centrin with the pericentriolar material (PCM) marker pericentrin. A total of 100 interphase mononucleated cells were examined under all experimental conditions. Since cell cycle markers were not used for co-staining, only cells displaying more than four centrioles, as indicated by centrin staining, were considered to have centrosome amplification (CA).

### **2.4.6 Analysis of EMT Markers**

Three EMT markers were assessed: E-cadherin, Vimentin, and Fibronectin. IF microscopy permitted the analysis of these markers' expression within the cells. This method allows for the evaluation of localization/distribution patterns. Sum intensity

projection images were used for fluorescent intensity measurements. These were prepared using Image J software (National Institutes of Health).

## **2.5 Enzyme-linked immunosorbent assay (ELISA)**

Following transfection and 72 hours of incubation, cell media was replaced by serum-free plain MCDB-153 cell culture media for 22 hours. This conditioned media was then collected and centrifuged at 1100 rpm for 3 min to obtain cell-free supernatant, which was immediately aliquoted and snap-frozen for subsequent analysis. Secreted levels of fibronectin were measured using the Human FN1 ELISA Kit (Invitrogen) following the manufacturer's protocol.

## **2.6 Statistical analysis**

The number of independent biological replicates performed for each assay is indicated in the corresponding figure legend. Results are presented as the mean  $\pm$  standard error of the mean (SEM). Statistical analyses were performed using ordinary one-way ANOVA for multiple comparisons and the unpaired Student's t-test, utilizing the GraphPad Prism 8.0 statistical software package (GraphPad Prism 8.0.2). A p-value of less than 0.05 was considered statistically significant for all analyses.

# **3. Results**

In Barrett's esophagus (BE) progression, centrosome amplification (CA) has been reported to arise as early as metaplasia and increase significantly in dysplasia<sup>27</sup>. Moreover, it was only detected in BE metaplastic tissue of patients that progressed into neoplasia<sup>27</sup>. Extra centrosome numbers have been shown to promote features of malignant transformation and tumorigenesis, like more migratory and invasive potentials<sup>54,57,72,77</sup>. Given that dysplasia cells have higher migration and invasion potential than metaplasia cells<sup>27,29</sup>, we hypothesized that CA could be responsible for this malignant gain in dysplasia.

### 3.1 The impact of reducing CA in the migratory and invasiveness capacity of dysplasia cells

To test the hypothesis mentioned above, we designed an assay in which we would reduce the CA levels of dysplasia cells, where CA levels are naturally high, and then test whether their migratory and/or invasiveness capacity was affected (Figure 3.1).

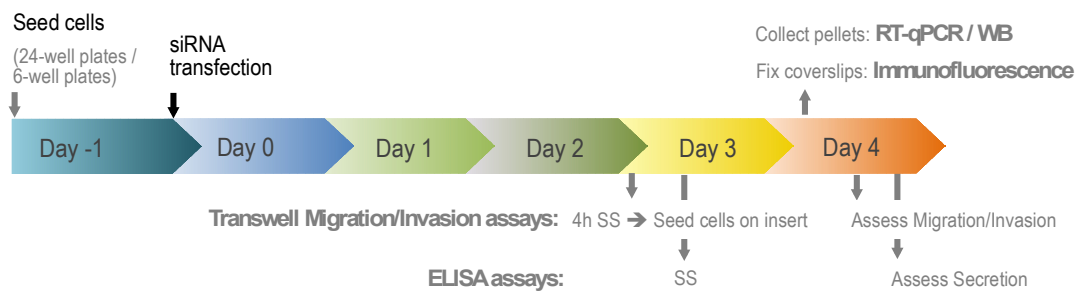


**Figure 3.1 - Schematic representation of the experimental layout.** To assess the impact of centrosome amplification in migration and invasion in dysplasia, dysplasia CP-D cells transfected with control (GL2), PLK4, or SAS6 siRNA were submitted to transwell migration and invasion assays. Effective depletion of either PLK4 or SAS6 was assessed by RT-qPCR and western blot. Reduction of centrosome amplification levels was confirmed by immunofluorescence. ELISA assays were used to assess changes in these cell's secretome.

To reduce CA levels in dysplasia, we depleted key proteins of centriole formation, PLK4 or SAS6, through small interference RNA (siRNA). By impeding the cells' capacity to replicate their centrosomes normally, we will suppress the generation of new centrosomes, and the existing supernumerary centrosomes will be diluted in the cell population through successive cell divisions, ultimately leading to an overall decrease in the incidence of CA<sup>30</sup>. Preliminary studies from our laboratory (data not shown) showed that this approach successfully reduced the level of CA in all three cell lines representative of BE high-grade dysplasia<sup>97</sup>, which inherently exhibit similar levels of CA and lost WT-p53<sup>27</sup>. Importantly, those preliminary results showed that CA levels were reduced after three days of siRNA transfection of either *PLK4* or *SAS6* and that this was maintained after four days<sup>97</sup>.

To assess dysplasia cells' migratory and invasiveness capacity, we used classic transwell migration or invasion assays<sup>98</sup>. The migration transwell assay measures cell movement through pores towards a chemoattractant, while the invasion test evaluates cells' ability to degrade a matrix barrier. The invading cells are stained and quantified.

These assays assess the cells' ability to move or invade through a matrix, a key property related to cancer metastasis.

To ensure that CA reduction was maintained throughout the transwell migration and invasion assays, they were only carried out three days after transfection and analyzed 22 hours later (i.e., four days after siRNA transfection) (Figure 3.1).

### 3.1.1 Depletion of *PLK4* or *SAS6* leads to a significant decrease of CA in dysplasia cells

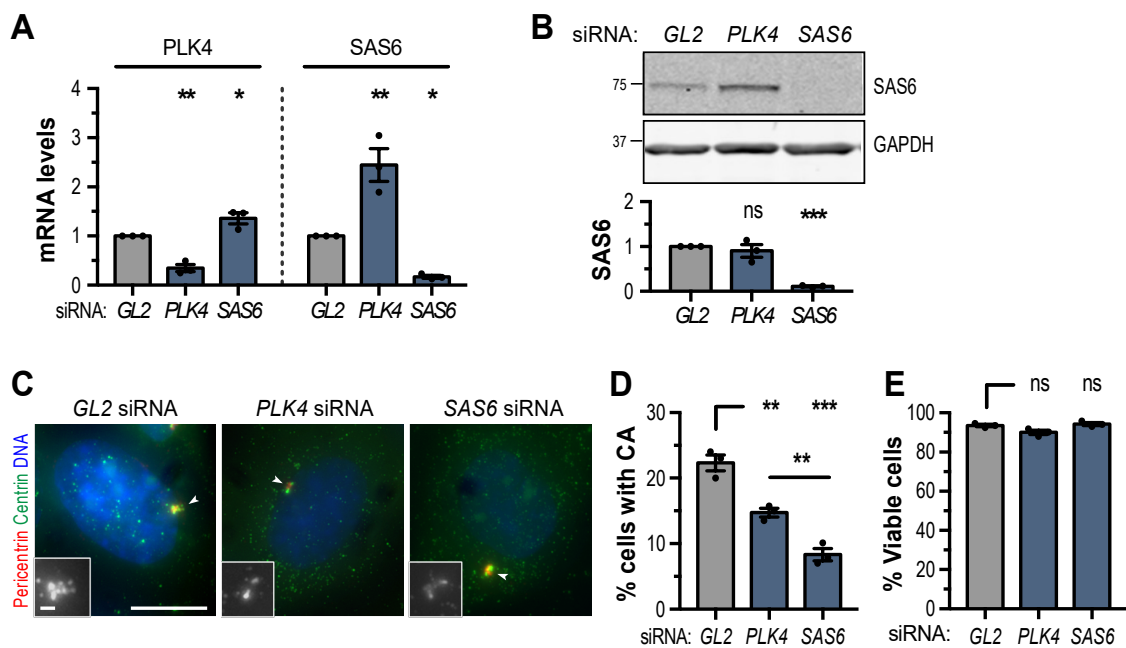


**Figure 3.2 - Depletion of key proteins for centrosome formation reduces levels of centrosome amplification (CA) in dysplasia cells.** Dysplasia cells were transfected with control (*GL2*), *PLK4* or *SAS6* siRNA. (A) Levels of *PLK4* and *SAS6* mRNA transcripts were assessed by RT-qPCR. Histogram shows *PLK4* or *SAS6* quantification relative to the control (*GAPDH*); ratios were normalized to levels in control cells. (B) *SAS6* protein levels were assessed by western blot. Histogram shows quantification relative to the loading control (*GAPDH*); ratios were normalized to the levels in control cells. Representative image is shown. (C-D) Cells were stained for centrioles (centrin, green), PCM (pericentrin, red) and DNA (blue). (C) Representative merged images are shown. Insets show enlargements of centrioles, as indicated by the arrows. Scale bars: 10  $\mu\text{m}$  (main images), 1  $\mu\text{m}$  (insets). (D) Quantification of cells with centrosome amplification.  $n=100$  cells/condition/experiment. (E) Quantification of cellular viability. Histograms depict means  $\pm$  SEM of three independent experiments. ns, not significant; \*,  $P<0.05$ ; \*\*,  $P<0.01$ ; \*\*\*,  $P<0.001$  (ANOVA).

To investigate the effectiveness of *PLK4* or *SAS6* depletion, we assessed the mRNA and protein levels of these molecules using reverse transcriptase quantitative Real-Time Polymerase Chain Reaction (RT-qPCR) and western blot.

RT-qPCR analysis revealed that the *PLK4* and *SAS6* mRNA levels were significantly reduced in dysplasia cells transfected with *PLK4*-siRNA or *SAS6*-siRNA, respectively (Figure 3.2 A). Importantly, western blot analysis also confirmed that *SAS6* depletion was efficient at the protein level (Figure 3.2 B). Given the overall low protein levels of *PLK4*, we did not evaluate its depletion by western blot. Intriguingly, the depletion of each molecule seemed to affect the mRNA levels of the other compared to the control group, suggesting a potential counteracting mechanism (Figure 3.2 A). Notably, *SAS6*-siRNA resulted in significantly high levels of *PLK4* mRNA and vice versa. However, the increase in *SAS6* mRNA levels upon *PLK4*-siRNA was insufficient to elevate *SAS6* protein levels (Figure 3.2B), suggesting that these changes at the transcriptional levels may not be reflected at the transduction level. These results confirm that *PLK4*-siRNA and *SAS6*-siRNA can effectively deplete their respective targeting molecules in dysplasia cells.

To ensure that the incidence of CA was diminished upon *PLK4* or *SAS6* depletion, we assessed centriole numbers in a cell-by-cell manner using IF microscopy, a method optimized in our laboratory (please see Methods for a detailed description of centriole scoring). To ensure we scored true centrioles, we counted the number of centrioles (marked by centrin) co-localized with the PCM protein Pericentrin (Figure 3.2C) in each cell. Only cells with more than four centrioles were deemed to have CA. As expected, the depletion of either *PLK4* or *SAS6* led to a significant reduction in the percentage of cells with CA compared to control cells (Figure 3.2 D). Interestingly, *SAS6*-depletion appears to lead to a more efficient reduction in CA levels than *PLK4*-depletion. To ensure that the reduction in the incidence of cells with CA did not result from reduced viability of *PLK4*- or *SAS6*-depleted cells, we assessed these cells' viability after the four days of transfection. Here, we found that neither *PLK4* nor *SAS6* depletion affected the viability of dysplasia cells (Figure 3.2E). Together, these results show that depletion of *PLK4* or *SAS6* efficiently reduces CA levels in dysplasia cells.

In conclusion, these results show that depleting either *PLK4* or *SAS6* successfully reduces the levels of CA in dysplasia cells. By investigating the impact of reducing CA in these cells using the two depletions in parallel, we can more accurately determine if a given observed effect is indeed the result of CA reduction and not only the result of specific changes in one of these molecules.

### 3.1.2 Reduction of CA levels decreases the migratory and invasive capacity of dysplasia cells

To investigate the impact of reducing CA on dysplasia cells' capabilities to migrate or invade, we used classic transwell Boyden chamber assays. In both assays, serum-starved cells are resuspended in serum-free media and placed on the top side of a chamber with small pores through which cells can migrate toward the bottom side of the chamber filled with full media that serves as a chemo-attractant. Given that the cells were serum-starved, it is expected that the complete media in the lower chambers would promote cell mobility<sup>98</sup>. In the transwell invasion assay, a matrigel layer is additionally incorporated on the porous membrane, mimicking the ECM, which only allows the passage of cells exhibiting invasive capabilities, such as the ability to produce matrix-degrading enzymes (like MMPs)<sup>18,57</sup>. Analysis of the number of cells that have migrated into the lower chamber shows that *PLK4*- or *SAS6*-depleted cells show statistically significant reduced migratory capacity (Figure 3.3 A, B). Both depletions led to significantly lower invasion rates in the invasion tests. Although *SAS6* depletion resulted in a more efficient reduction of CA (Figure 3.2D) we did not observe a differential impact on dysplasia cells' migration or invasion rates (Figure 3.3 B).

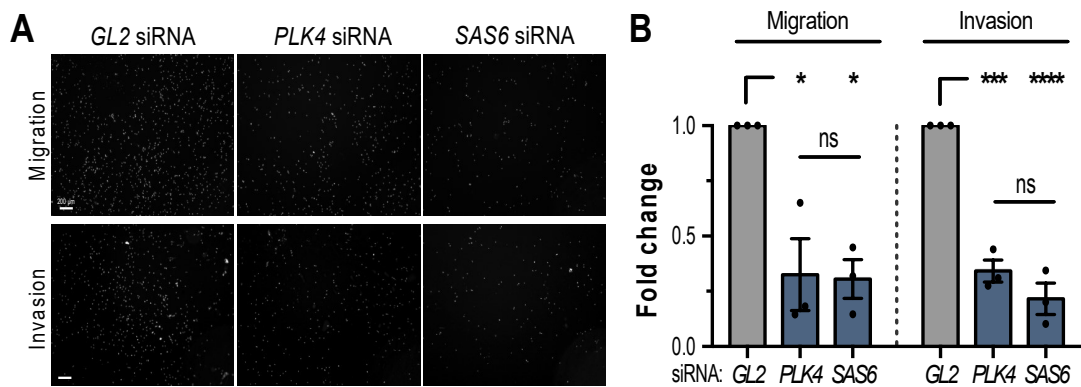


**Figure 3.3 - Dysplasia cells' migration and invasion capacity lessens with the decrease of CA levels.** Dysplasia cells transfected with control (*GL2*), *PLK4* or *SAS6* siRNA were submitted to transwell migration and invasion assays. Migrated/invaded cells were stained for DNA. (A) Representative images are shown. Scale bar: 200  $\mu$ m. (B) Quantification of the migrated or invaded cells relative to control cells. Histograms depict means  $\pm$  SEM of three independent experiments. ns, not significant; \*,  $P < 0.05$ ; \*\*\*,  $P < 0.001$ ; \*\*\*\*,  $P < 0.0001$

These results indicate that reducing the number of extra centrosomes decreases dysplasia cells' migratory and invasive potential.

## **3.2 The impact of reducing CA in the EMT features of dysplasia cells**

We then investigated the mechanisms underlying CA's role in migratory and invasiveness capacity in dysplasia.

In carcinogenesis, epithelial cells often undergo an epithelial-to-mesenchymal transition (EMT). This is a process that occurs in normal and pathological states and is often correlated to the gain of malignant traits<sup>73,75,99</sup>. In this transition, cells lose their characteristic epithelial properties by downregulating epithelial genes like E-cadherin and instead adopt mesenchymal cell features by upregulating mesenchymal genes such as vimentin, fibronectin, and MMPs<sup>29,55,77,100</sup>. This enables cells to migrate and invade other tissues, ultimately facilitating the metastatic process<sup>27,55,73</sup>.

In agreement with this, while metaplasia cells exhibit an epithelial phenotype, dysplasia cells exhibit mesenchymal features: increased motility and invasiveness capacity, accompanied by decreased levels of E-cadherin and increased vimentin and fibronectin<sup>27,29,70,100</sup>. Since the EMT process is reversible, we hypothesized that CA reduction in dysplasia cells led to a reduced migratory and invasiveness potential via alterations in EMT. Hence, we assessed mesenchymal and epithelial features in these cells to determine if CA reduction led to an EMT reversal in dysplasia.

### **3.2.1 Global mRNA and protein levels of EMT markers upon CA reduction**

To analyze alterations of EMT features in dysplasia, we first examined the mRNA and protein levels of three EMT markers after CA reduction by RT-qPCR and Western blot, respectively. Specifically, we assessed the levels of E-cadherin, vimentin, and fibronectin, which are commonly used in molecular analysis of EMT.

Analysis of mRNA levels showed that E-cadherin significantly increases upon depletion of PLK4 but not of SAS6 (Figure 3.4 A). In contrast, vimentin significantly increased upon SAS6 depletion but not PLK4 depletion (Figure 3.4A). Fibronectin levels, on the other hand, did not show any significant difference upon PLK4 or SAS6 depletion when compared to control cells (Figure 3.4 A).

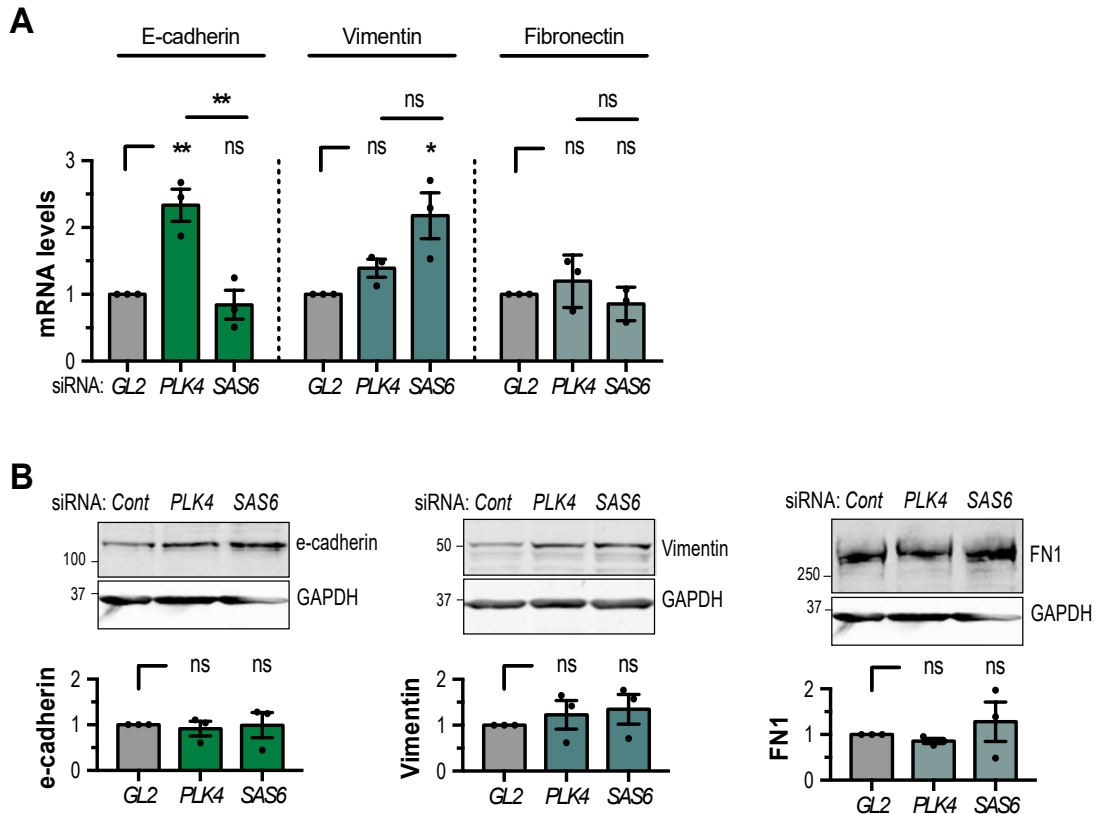


**Figure 3.4 - Dysplasia cells with reduced CA levels exhibit a hybrid EMT phenotype.** Dysplasia cells were transfected with control (*GL2*), *PLK4* or *SAS6* siRNA. (A) Levels of E-cadherin, vimentin and fibronectin mRNA transcripts were assessed by RT-qPCR. Histogram shows quantifications relative to the control (GAPDH); ratios were normalized to the levels in control cells. (B) E-cadherin, vimentin and fibronectin protein levels were assessed by western blot. Histograms show quantifications relative to the loading control (GAPDH); ratios were normalized to the levels in control cells. Representative images are shown. Histograms depict means  $\pm$  SEM of three independent experiments. ns, not significant; \*,  $P < 0.05$ ; \*\*,  $P < 0.01$  (ANOVA).

Analysis of protein levels revealed that despite some changes detected before at the mRNA level, E-cadherin and vimentin protein levels did not significantly change upon *PLK4* or *SAS6* depletion compared to control cells (Figure 3.4 B). Regarding fibronectin, we found some variability in the protein levels detected upon *SAS6* depletion. However, no statistically significant differences were found upon *PLK4* or *SAS6* depletion (Figure 3.4B). So, despite the levels of some molecules appearing to vary between experiments, these changes were either not statistically significant and/or did not occur for both *PLK4* or *SAS6* depletions.

In summary, these results indicate that reducing CA does not cause significant alterations in ETM markers.

### 3.2.2 Analysis of the impact of CA reduction in EMT markers by IF

To examine these markers in more detail, we assessed them by IF. This approach would allow us to i) examine localization/distribution patterns on a cell-by-cell basis and ii) measure intensity levels.

#### 3.2.2.1 E-cadherin and vimentin

E-cadherin is a transmembrane protein of the adherents junction, important in junctional barrier function in most epithelia, including that of the esophagus<sup>101</sup>. Upon Barrett's progression from metaplasia to dysplasia, E-cadherin has been reported to become less expressed<sup>29</sup>. Therefore, we first examined whether E-cadherin localization in dysplasia cells was altered upon CA reduction. This detailed localization analysis revealed that PLK4 knockdown increased the presence of E-cadherin in the cell

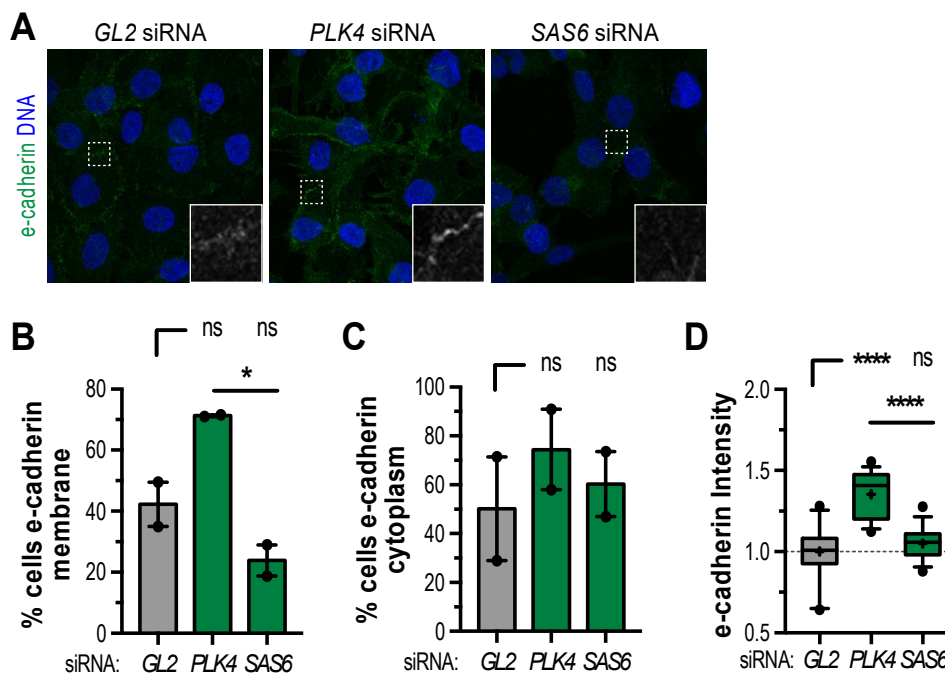


**Figure 3.5 - Impact of CA reduction on E-cadherin.** Dysplasia cells were transfected with control (GL2), PLK4 or SAS6 siRNA. Cells were stained for E-cadherin (green) and DNA (blue). (A) Representative merged images. Insets show enlargements of cellular membranes at inter-cellular contacts. Scale bar: 10 $\mu$ m. (B) Quantification of cells with E-cadherin at the cell membrane. (C) Quantification of cells with E-cadherin accumulated in the cytoplasm. (D) Quantification of E-cadherin overall intensity. Histograms depict means  $\pm$  SEM of two independent experiments. ns, not significant; \*,  $P < 0.05$ ; \*\*\*\*,  $P < 0.0001$  (ANOVA).

membrane (Figure 3.5 A, B) and a trend towards increased levels in the cytoplasm (Figure 3.5 A, C).

In contrast, depletion of SAS6 was associated with a trend of lower levels of membrane-bound E-cadherin (though not statistically significant), while cytoplasmic expression remained unchanged (Figure 3.5 B, C). Overall intensity measurements revealed that indeed E-cadherin intensity levels increased following PLK4 depletion, whereas no significant changes were observed upon SAS6 depletion (Figure 3.5D).

Vimentin is a type III intermediate filament protein expected to be in the cytosolic portion of cells expressed in normal mesenchymal cells. Overexpression of vimentin is frequently associated with increased migratory/invasive capacity of cancer cells<sup>102</sup>. In BE progression from metaplasia to dysplasia, vimentin has been reported to increase its expression<sup>29</sup>. Accordingly, as expected, vimentin was expressed mainly in the cytoplasm surrounding the nucleus in all conditions (Figure 3.6A). Not all cells visibly contained vimentin. Although there was a detectable trend in the increased number of cells expressing vimentin upon depletion of either PLK4 or SAS6, these were not statistically significant (Figure 3.6 B).

Overall, this analysis shows that although the epithelial marker E-cadherin was raised upon PLK4 depletion, this was not seen upon SAS6 depletion. We thereby exclude that reduction of CA as the probable cause for that increase. As for the mesenchymal marker vimentin, seeing that a slight increase in its expression was detected upon depletion of either PLK4 or SAS6, this analysis suggests that such changes could

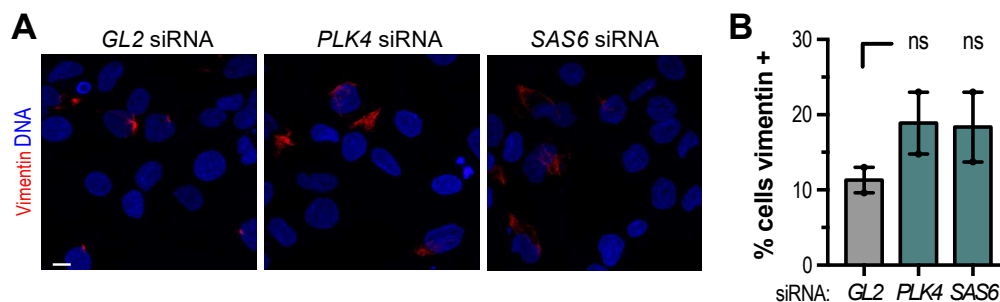


**Figure 3.6 - Impact of CA reduction on vimentin.** Dysplasia cells were transfected with control (*GL2*), *PLK4* or *SAS6* siRNA. Cells were stained for vimentin (red) and DNA (blue). **(A)** Representative merged images are shown. Scale bar: 10 $\mu$ m. **(B)** Quantification of cells with vimentin. Histogram depicts means  $\pm$  SEM of two independent experiments. ns, not significant (ANOVA).

result from reduced CA.

### 3.2.2.2 Fibronectin

Fibronectin plays crucial roles in cell adhesion, wound healing, tissue morphogenesis, cell migration, and signal transduction<sup>86,103</sup>. These functions make fibronectin integral to both normal physiology and disease progression. Fibronectin is also a mesenchymal marker used to identify EMT<sup>29</sup>. It is commonly localized in the ECM and appears as a fibrillar network around cells, especially in areas where cell adhesion and migration occur. In tissue samples, fibronectin is found in the basement membrane and interstitial connective tissue, indicating its role in providing structural support and influencing cell behavior<sup>87</sup>.

Our initial assessment of fibronectin by IF suggested increased intracellular fibronectin upon PLK4 or SAS6 depletion. To guarantee that the detection of fibronectin by immunofluorescence was specific, we compared this with cells depleted of fibronectin. Therefore, we first validated fibronectin depletion efficiency through siRNA (*FN1*-siRNA). Indeed, analysis of mRNA and protein levels of fibronectin by RT-qPCR and western blot showed that fibronectin was efficiently depleted in dysplasia cells (Figure 3.7 A, B) and that its depletion had no impact on cellular viability (Figure 3.7 C). We then proceeded with a careful examination of fibronectin by IF. Indeed, upon *FN1*-siRNA, fibronectin was not detected, whereas in *PLK4*- and *SAS6*-siRNA treated cells, fibronectin intensity was higher than in control cells. (Figure 3.8A, B).

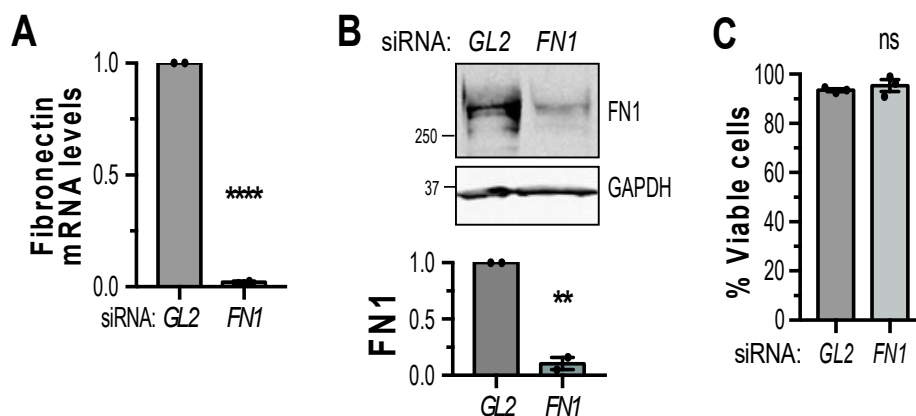


**Figure 3.7 - Depletion of fibronectin in dysplasia cells.** Dysplasia cells were transfected with control (*GL2*) or *FN1* siRNA. (A) Levels of fibronectin in mRNA transcripts were assessed by RT-qPCR. Histogram shows quantification relative to the control (GAPDH); ratios were normalized to the levels in control cells. (B) Fibronectin protein levels were assessed by western blot. The histogram shows quantification relative to the loading control (GAPDH); ratios were normalized to the levels in control cells. (C) Quantification of cellular viability. Histograms depict means  $\pm$  SEM of two (A-B) or three (C) independent experiments. ns, not significant; \*\*,  $P < 0.01$ ; \*\*\*,  $P < 0.001$ ; \*\*\*\*,  $P < 0.0001$  (ANOVA).

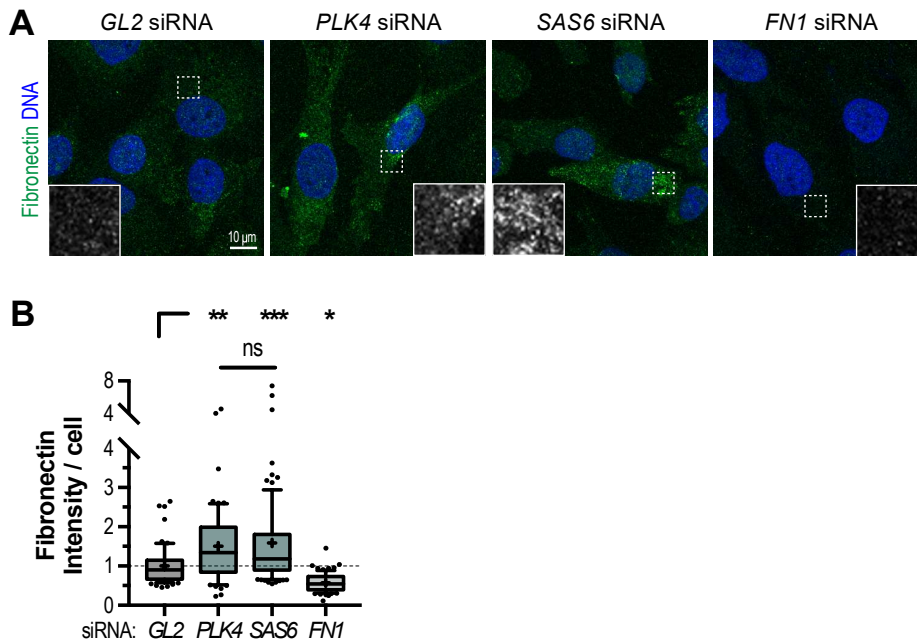


**Figure 3.8 - Impact of CA reduction on fibronectin.** Dysplasia cells were transfected with control (*GL2*), *PLK4*, *SAS6* or *FN1* siRNA. Cells were stained for fibronectin (green) and DNA (blue). **(A)** Representative merged images. Insets show enlargements of indicated areas. Scale bar: 10 $\mu$ m. **(B)** Quantification of fibronectin intracellular intensity. Histograms depict means  $\pm$  SEM of three independent experiments. ns, not significant; \*,  $P < 0.05$ ; \*\*,  $P < 0.01$ ; \*\*\*,  $P < 0.001$  (ANOVA).

Collectively, the analysis of the EMT panel suggests that reducing CA in dysplasia does not lead to an EMT reversal. Rather, we found that CA reduction could impact fibronectin intracellular levels.

Knowing that fibronectin has been linked to cancer progression<sup>86,92,95,104–106</sup>, we investigated whether these changes in fibronectin levels were due to reducing CA and if they affected the migratory and invasive capabilities of dysplastic esophageal cells.

### 3.3 The impact of reducing CA on fibronectin and its role in cell invasion

Besides being a mesenchymal marker, fibronectin is also an important component of the ECM<sup>86,89,94</sup>. Indeed, previous studies have reported that fibronectin is an important contributor to migration and invasiveness<sup>86,89,92,105</sup>. Moreover, when its secretion is altered, fibronectin seems to hamper cell invasion by accumulating intracellularly in vesicles<sup>86,92</sup>.

Despite no changes in fibronectin mRNA levels (Figure 3.4 A) our results show that fibronectin protein levels detected inside cells by IF increased (Figure 3.8 B). This

suggests that the accumulation of fibronectin is not due to its increased biosynthesis but rather to hampered fibronectin secretion into the extracellular space.

Accordingly, we hypothesize that CA may contribute to invasiveness in dysplasia by promoting fibronectin secretion. If this is correct, we would expect that (i) reducing CA in dysplasia would result in reduced fibronectin levels present in the extracellular space and (ii) the absence of fibronectin would be sufficient to reduce the invasiveness potential of dysplasia cells.

### 3.3.1 Impact of CA reduction on fibronectin secretion into extracellular space

To demonstrate that CA reduction decreases fibronectin secretion into the extracellular space, we conducted ELISA assays to examine fibronectin levels in the extracellular media upon depletion of either PLK4 or SAS6. As a positive control, we assessed secreted fibronectin levels in *FN1*-siRNA treated dysplasia cells.

As expected, the ELISA results show that the absence of fibronectin upon its depletion caused a total decrease in fibronectin levels in the culture medium (Figure 3.9). Moreover, and in agreement with our hypothesis, there is a significant decrease in fibronectin secretion levels for both PLK4- and SAS6-depleted cell populations, demonstrating that reducing CA reduces fibronectin extracellular secretion.

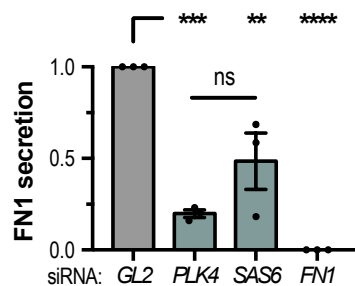


**Figure 3.9 - Dysplasia cells show decreased fibronectin secretion upon CA reduction.**

Dysplasia cells were transfected with control (*GL2*), *PLK4*, *SAS6*, or *FN1* siRNA. Histogram shows quantification of fibronectin in the extracellular space, which was assessed by ELISA; ratios were normalized to the levels in control cells. Histogram depicts means  $\pm$  SEM of three independent experiments. ns, not significant; \*,  $P < 0.05$ ; \*\*,  $P < 0.01$ ; \*\*\*,  $P < 0.001$ , P (ANOVA).

### 3.3.2 Impact of reducing fibronectin secretion in dysplasia cells' migratory and invasiveness capacity

Finally, to determine the impact of reducing fibronectin secretion on dysplasia cells' migration and invasion potentials, we proceeded with another set of transwell migration

and invasion assays on fibronectin-depleted cells. These results suggest a trend where fibronectin depletion may lead to a slight decrease in migration. However, this was not statistically significant (Figure 3.10 A, B). On the other hand, the depletion of fibronectin led to a significant decrease in the invasiveness capacity of dysplasia cells (Figure 3.10 A, B).

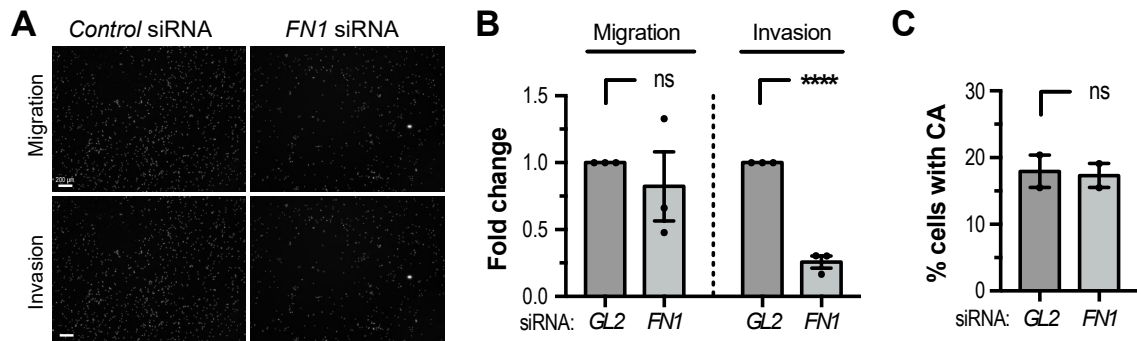


**Figure 3.10 - Dysplasia cells' invasion capacity lessens with the depletion of fibronectin.** Dysplasia cells transfected with control (*GL2*) or *FN1* siRNA were submitted to transwell migration and invasion assays. Migrated/invaded cells were stained for DNA. (A) Representative images are shown. Scale bar: 200  $\mu$ m. (B) Quantification of the migrated or invaded cells relative to control cells. (C) Quantification of cellular viability. Histograms depict means  $\pm$  SEM of two (C) or three (A-B) independent experiments. ns, not significant; \*\*\*\*,  $P < 0.0001$  (ANOVA).

These assays show that siRNA depletion of fibronectin recapitulated the effects of CA reduction in dysplasia cells' invasiveness potential. Therefore, these results suggest that decreased fibronectin secretion, rather than its cytosolic accumulation, underlies its contribution to the reduction in invasion rates.

To check if fibronectin depletion did not affect centrosome numbers, we counted centriole numbers in *FN1*-siRNA treated cells using IF. This analysis confirmed that fibronectin depletion alone does not reduce CA levels in dysplasia (Figure 3.10 C). So, despite having high CA levels, fibronectin-depleted cells also displayed decreased invasive capabilities. This suggests that fibronectin is a downstream factor of CA and that its secretion is important for the CA-mediated invasion capacity in dysplasia. On the other hand, seeing that fibronectin-depleted cells, which harbored high CA levels, still appeared to preserve their migratory capacity, these results suggest that CA-mediated migratory capacity in dysplasia is independent of fibronectin.

## 4. Discussion

In Barrett's esophagus (BE) multistep malignant progression, the stage preceding invasive esophageal adenocarcinoma (EAC) – dysplasia – is a very important event as its diagnosis is used to signal patients who have a high risk of progressing to EAC. The latest American College of Gastroenterology guidelines update<sup>8</sup> emphasizes the lack of robust evidence supporting biomarkers for personalized treatment strategies. Gaining a deeper understanding of the molecular and cellular changes occurring at the dysplastic stage, where progression to EAC is driven, is essential for developing strategies that can be routinely implemented in clinical practice for risk stratification and management of BE.

Centrosome amplification (CA), which occurs in tumorigenesis of several organs<sup>27,35,54,72,92</sup> and is known to contribute to cell invasion<sup>37,50,62</sup> is a prominent feature in BE dysplasia<sup>27</sup>. However, whether and how CA impacts dysplasia cells' migratory and invasive potential in BE progression has not been clarified. This work demonstrates that reducing the incidence of CA levels in dysplastic cells is sufficient to reduce their pro-tumorigenic traits of migration and invasion. We also provide data showing that dysplasia cells harboring supernumerary centrosomes promote this aggressive phenotype, not necessarily by undergoing an epithelial-to-mesenchymal transition (EMT) but specifically by altering fibronectin secretion.

In this study, we sought to reduce centrosome numbers by targeting the expression of two key proteins involved in centriolar biogenesis<sup>30,47</sup>. Through the use of two independent siRNA oligonucleotide transfections, we successfully achieved the transient depletion of either PLK4 or SAS6, resulting in the suppression of supernumerary centrosomes. By studying these two molecules in parallel, we could test if the observed effects were indeed the result of reduced CA levels rather than due to the specific interference in a specific molecule alone, such as PLK4<sup>55,77,107,108</sup>. Interestingly, we observed a compensatory mechanism at the mRNA level wherein PLK4 depletion led to elevated SAS6 levels. Conversely, SAS6 depletion increased PLK4 levels compared to control groups, suggesting a regulatory feedback loop between PLK4 and SAS6. Literature shows that PLK4 levels are tightly regulated<sup>46,47,109</sup>, and feedback mechanisms between PLK4 and SAS6 activity contribute to the control of centriole duplication<sup>46,109</sup>. Therefore, we speculate that the depletion of PLK4 and SAS6 may induce a compensatory interplay, which could mitigate the impact of reduced protein levels within the cells. Despite this potential

compensatory response, which may result in variable levels of CA reduction in dysplastic cells, both depletion of PLK4 or SAS6 lead to a significant reduction in the levels of CA in dysplasia cells. It is also important to note that while other studies have scored centrosome numbers using solely PCM markers such as pericentrin or  $\gamma$ -tubulin<sup>27,49,110</sup>, we decided to mark both pericentrin, a PCM marker, and centrin, a centriolar marker, to be more specific in identifying true centrosomes and avoid over- or underestimating the centrosome counts. Cells with more than four centrioles were considered to exhibit CA. Additionally, by confirming that cell viability was not compromised upon depletion of either PLK4 or SAS6, we ruled out the possibility that observed differences in migration or invasion were due to cell loss caused by depletion-induced toxicity.

To examine the impact of CA reduction on the migration and invasion potential of dysplasia cells, we chose to use classic transwell Boyden Chamber assays because they have been previously used to study these BE dysplasia cell lines<sup>29</sup> and are widely used in other studies using cancer cell lines, including breast<sup>52,57,66,107</sup>, prostate<sup>92</sup>, colon<sup>55,77</sup> and even BE progression cell models<sup>111</sup>. Here, we show that depletion of either PLK4 or SAS6 leads to decreased migration and invasion rates in dysplasia cells. This strongly supports the notion that CA contributes to promoting these malignant characteristics in dysplasia, reinforcing the role of centrosome regulation in modulating cellular behaviors linked to tumorigenesis. The literature shows that manipulation of PLK4 levels has been more extensively used than SAS6 to induce or reduce CA in several cell lines. Nevertheless, in different cell models from various organs, changes in the levels of these centriolar biogenesis proteins have been shown to affect their invasion and migratory capabilities<sup>55,57,72,77</sup>.

While strong evidence demonstrates that CA contributes to cell migration and invasion capabilities, their underlying mechanisms are not yet entirely clear. Dysplastic cells exhibit a mesenchymal phenotype, which favors increased migratory and invasive potential<sup>29,100</sup>. Furthermore, during cancer progression, cells frequently undergo an epithelial-to-mesenchymal transition (EMT) to acquire malignant traits<sup>75</sup>. EMT is initiated by the loss of epithelial junctions and cell polarity, which results in cytoskeleton reorganization and a rise of a predominantly mesenchymal phenotype occurring in gradual steps<sup>73,75</sup>. This involves the loss of the epithelial marker E-cadherin and increases in mesenchymal markers (e.g., vimentin and fibronectin) and matrix metalloproteinases (MMPs)<sup>18</sup>, facilitating cell migration, invasion, and extracellular matrix degradation<sup>18,75</sup>. Given the reversibility of EMT, we investigated whether a reduction in centrosome amplification could reverse this transition, driving dysplasia

toward a less mesenchymal phenotype, which could help explain the lessening of the migratory and invasive traits. Our data surprisingly showed that reducing CA creates changes; however, they either do not occur significantly in parallel for PLK4 or SAS6 depletions (e-cadherin and vimentin mRNA levels), excluding CA as the cause, or they are not statistically significant (e-cadherin and vimentin overall protein levels; fibronectin mRNA and overall protein levels). Furthermore, the variability observed between the technical replicates implies a cautious interpretation of the results, impeding our ability to classify these changes as part of an EMT reversal. Although initially it could appear incongruent to witness the occurrence of epithelial and mesenchymal markers together, this has been reported as a hybrid EMT phenotype<sup>29,107</sup>. Hybrid states appear in the early stages of tumorigenesis, helping cells develop migration, invasion, and stemness<sup>99</sup>. Here, we found that although dysplasia cells exhibit a potential hybrid EMT phenotype when CA is reduced, they do not present an increased migration and invasion potential.

This motivated the need for a more refined cell-by-cell observation of EMT markers by IF. Using this method, we could examine localization/distribution patterns and measure the intensity levels of EMT markers. Similarly to what we observed for mRNA levels, although the overall intracellular E-cadherin levels significantly increased upon PLK4 depletion, they were unchanged upon SAS6 depletion. Although the rise in E-cadherin intensity was expected in an EMT reversal, these findings only happen upon PLK4 depletion, suggesting once more that CA is not the factor responsible for the rise in intensity. It would be interesting to address the role of PLK4 in E-cadherin regulation. Other studies in breast cancer cells have linked the loss of E-cadherin function to an increased tolerance for CA via centrosome clustering<sup>76</sup>. The researchers hypothesized that the proximity of centrosomes in cells lacking E-cadherin facilitates efficient centrosome clustering, a process crucial for the survival of cancer cells with supernumerary centrosomes. This implies that the loss of E-cadherin may serve as a strategy cancer cells utilize to manage the challenges associated with excess centrosomes<sup>76</sup>. While the E-cadherin loss aligns with our findings, further investigation is necessary to validate if this mechanism could contribute to centrosome invasive and migratory potential. Additionally, although PLK4 appears to influence E-cadherin expression, which may contribute to the observed decrease in migration and invasion upon PLK4 depletion, this is not observed upon SAS6 depletion and, therefore, does not explain the reduction in migration and invasion upon CA reduction (i.e., upon either PLK4 or SAS6 depletion). Therefore, there must be other mechanisms underlying CA's

role in migration and invasion, and further assay investigation is recommended to clarify the potential role of E-cadherin in this context.

Despite the observed reduction in migratory and invasive capacities following the decrease in centriole numbers, which is typically associated with the downregulation of mesenchymal markers<sup>29,72,74</sup>, it was unexpected that vimentin levels remained unchanged. Regarding fibronectin expression, on the other hand, IF analysis yielded noteworthy and puzzling findings. Unlike what we expected to find if there was a reversal in EMT phenotype in dysplasia cells upon CA reduction, we found a marked cytosolic accumulation of fibronectin marker following PLK4 or SAS6 depletion. So, together, these results indicated that the reduction of CA in dysplasia was not accompanied by a reversal of the EMT phenotype. Still, our observations that CA reduction may impact fibronectin localization and expression warranted further investigation into the underlying mechanisms.

Fibronectin is not only a mesenchymal marker but also a crucial component of the ECM, mediating several cellular functions, particularly invasion<sup>18,88,94</sup>. Interestingly, the accumulation of intracellular fibronectin detected by IF contrasted with the unchanged fibronectin protein levels detected by western blot. Moreover, the variability observed between experiments led us to interrogate our methods and realize a limitation of our approach. To detach cells from the wells, we used a trypsin-based reagent. This was immediately washed out after cell pellet collection and before cell lysis. As this enzymatic reagent degrades proteins responsible for cell attachment, it also breaks several extracellular protein components, such as fibronectin. This likely led to a variable level of degradation of extracellular fibronectin upon cell collection, thus affecting the total levels (intra- and extracellular) of the detected fibronectin by western blot. This led us to realize that the cell detachment method was inappropriate for measuring proteins that localize both inside cells and in ECM. Therefore, it is recommended that future studies use alternative methods, such as cell scratching, to collect cells to analyze by western blot. However, it is important to note that this did not invalidate the intracellular assessment by IF.

Fibronectin overexpression in tumors supports tumor growth and metastasis by promoting cell adhesion, migration, and matrix assembly<sup>94</sup>. Notably, impaired fibronectin secretion can lead to its intracellular accumulation<sup>92</sup>, suppressing tumor progression<sup>104,106</sup> and chemoresistance<sup>112</sup>. Since the increase in intracellular fibronectin upon CA reduction was accompanied by no detectable changes in its mRNA levels, our observations suggested that the increased intracellular fibronectin

levels were not due to dysplasia cells' overproduction of this protein but rather to its accumulation due to reduced secretion. Indeed, ELISA tests done on the culture medium corroborated our hypothesis. These observations suggest that CA in dysplasia promotes fibronectin secretion. Fibronectin secretion allows for assembling a fibronectin-rich matrix<sup>87</sup>, providing structural support and a scaffold for cells, facilitating their adhesion and migration through the surrounding tissues. Fibronectin interacts with integrins on the surface of cells, which enhances cells', especially cancer cells, ability to adhere to the ECM, which is critical for their movement and invasion into adjacent tissues<sup>86,88</sup>. When cancer cells strongly adhere to the ECM, they can better utilize it as a scaffold for movement<sup>105</sup>. This is particularly important during invasion, when cells must migrate through the matrix to reach surrounding tissues or enter the bloodstream<sup>86</sup>.

In light of this, we then aimed to test if fibronectin secretion was needed for CA-mediated invasion in dysplasia. Indeed, we found that the absence of fibronectin is sufficient to significantly reduce the invasiveness potential of dysplasia cells. Since these fibronectin-depleted cells still contained elevated CA levels, our results indicate that CA-mediated fibronectin secretion is crucial for CA-mediated invasion in dysplasia. Previous studies investigating the role of centrosome amplification in breast cancer cells have shown that CA enhances migration and invasion by modulating the expression of key proteins, including integrin  $\beta$ -3 and its binding partner, fibronectin<sup>57</sup>. However, these studies primarily focus on protein expression levels rather than fibronectin secretion, which contrasts with our study's findings, which emphasize the importance of fibronectin secretion in invasion. Our results demonstrate that while fibronectin depletion did not significantly affect migration rates, it led to a marked reduction in invasion rates, suggesting that CA provokes ECM remodeling indirectly by altering signaling cascades. Mechanistically, we propose that in the context of CA reduction, less fibronectin is available in the ECM to form fibronectin-integrin binding, thus affecting the formation of focal adhesions and influencing actin cytoskeleton dynamics<sup>86</sup>, which are critical for cell motility<sup>91,105</sup>. Moreover, the lack of fibronectin-integrin binding can also impact signaling cascades that activate MMPs that remodel the ECM and facilitate cell movement<sup>74,88,89,95</sup>. Investigating how other molecules are influenced by the altered secretion of fibronectin resulting from CA would be beneficial. For example, it may be helpful to examine changes in molecules involved in fibronectin trafficking<sup>113</sup> or evaluate the expression of matrix metalloproteinases. By understanding these mechanisms, we may gain a clearer insight into how CA contributes to BE progression.

While CA-reduction in dysplasia clearly resulted in fibronectin accumulation inside cells and subsequent reduction in its secretion, it is still unclear in which subcellular structures fibronectin may be accumulated and how their cellular trafficking is being affected. The mechanisms underlying fibronectin regulation, particularly its processing, trafficking, and secretion, remain poorly understood<sup>86</sup>. Further investigation is needed to clarify the precise regulatory pathways governing fibronectin expression and secretion role in cancer progression. A study on prostate cancer cells suggested that cellular fibronectin co-localizes to the endosomes, particularly late endosomes identified by Rab7. This suggests that it is being processed for potential secretion but is retained due to the effects of Hsp90 inhibition<sup>92</sup>. Rabs are a small GTPases family responsible for coordinating endosome formation, movement, and fusion events<sup>114,115</sup>. Notably, centrosomes have been reported to affect endosome recycling pathways. Considering that Rab5, Rab7, and Rab11<sup>67,92,116,117</sup> serve as endosome markers — representing early endosomes and the degradation route—they should make well-suited candidates to test whether CA reduction leads to fibronectin accumulation in such endosomes. In the future, it will be important to dissect the mechanisms by which CA mediates fibronectin trafficking and secretion.

## **5. Conclusion and future perspectives**

This study demonstrated that centrosome amplification (CA) promotes the acquisition of invasive properties in Barrett's esophagus dysplastic cells in part by enhancing fibronectin secretion. Importantly, our findings also provided valuable insights into potential new mechanisms by which CA may contribute to Barrett's esophagus carcinogenesis, revealing novel pathways that will be further explored and may be translated into useful clinical tools in the future. Furthermore, by demonstrating the role of CA in Barrett's esophagus progression, this study supports the discovery and use of other molecules affected by those anomalies as part of a biomarker signature panel that facilitates the identification of Barrett's esophagus patients with an increased risk of disease progression. In turn, this could improve the targeted use of standard biopsy protocols. Finally, given the prevalence of CA in most human cancers, these insights may apply to other cellular models in other organs or pathways, suggesting potential future research directions.

## 6. References

1. Souza, R. F. & Spechler, S. J. Mechanisms and pathophysiology of Barrett oesophagus. *Nat. Rev. Gastroenterol. Hepatol.***19**, 605–620 (2022).
2. Stawinski, P. M., Dziadkowiec, K. N., Kuo, L. A., Echavarría, J. & Saligram, S. Barrett's Esophagus: An Updated Review. *Diagnostics (Basel, Switzerland)***13**, (2023).
3. Uhlenhopp, D. J., Then, E. O., Sunkara, T. & Gaduputi, V. Epidemiology of esophageal cancer: update in global trends, etiology and risk factors. *Clin. J. Gastroenterol.***13**, 1010–1021 (2020).
4. Liu, C. Q. *et al.* Epidemiology of esophageal cancer in 2020 and projections to 2030 and 2040. *Thoracic Cancer* vol. 14 3–11 at <https://doi.org/10.1111/1759-7714.14745> (2023).
5. Paris, S. & Souza, R. F. Pathophysiology of Gastroesophageal Reflux Disease: Epithelial Factors. *Esophagus Sixth Ed.* 376–393 (2021) doi:10.1002/9781119599692.ch22.
6. Naini, B. V., Souza, R. F. & Odze, R. D. Barrett's esophagus: A comprehensive and contemporary review for pathologists. *Am. J. Surg. Pathol.***40**, e45–e66 (2016).
7. Ekeke, C. N., Chan, E. G., Fabian, T., Villa-Sanchez, M. & Luketich, J. D. Recommendations for Surveillance and Management of Recurrent Esophageal Cancer Following Endoscopic Therapies. *Surg. Clin. North Am.***101**, 415–426 (2021).
8. Shaheen, N. J. *et al.* Diagnosis and Management of Barrett's Esophagus: An Updated ACG Guideline. *Am. J. Gastroenterol.***117**, 559–587 (2022).
9. Fitzgerald, R. C. *et al.* British Society of Gastroenterology guidelines on the diagnosis and management of Barrett's oesophagus. *Gut***63**, 7–42 (2014).
10. Sharma, P., Shaheen, N. J., Katzka, D. & Bergman, J. J. G. H. M. AGA Clinical Practice Update on Endoscopic Treatment of Barrett's Esophagus With Dysplasia and/or Early Cancer: Expert Review. *Gastroenterology***158**, 760–769 (2020).
11. Fabian, T. & Leung, A. Epidemiology of Barrett's Esophagus and Esophageal Carcinoma. *Surg. Clin. North Am.***101**, 381–389 (2021).
12. Geboes, K. & Hoorens, A. The cell of origin for Barrett's esophagus. *Science (80- )*.**373**, 737–738 (2021).
13. Read, M. D., Krishnadath, K. K., Clemons, N. J., Phillips, W. A. & Read MD, Krishnadath KK, Clemons NJ, P. W. Preclinical models for the study of Barrett's carcinogenesis. *Ann. N. Y. Acad. Sci.***1434**, 139–148 (2018).
14. Krishnadath, K. K. & Wang, K. K. Molecular pathogenesis of Barrett esophagus: current evidence. *Gastroenterol. Clin. North Am.***44**, 233–247 (2015).
15. Odze, R. D. Barrett esophagus: histology and pathology for the clinician. *Nat. Rev. Gastroenterol. Hepatol.***6**, 478–490 (2009).
16. Grady, W. M. & Yu, M. Molecular Evolution of Metaplasia to Adenocarcinoma in the Esophagus. *Dig. Dis. Sci.***63**, 2059–2069 (2018).
17. Rice, T. W., Patil, D. T. & Blackstone, E. H. 8th edition AJCC/UICC staging of cancers of

- the esophagus and esophagogastric junction: application to clinical practice. *Ann. Cardiothorac. Surg.***6**, 119–130 (2017).
18. Palumbo, A. *et al.* Esophageal Cancer Development: Crucial Clues Arising from the Extracellular Matrix. *Cells***9**, (2020).
  19. Whitson, M. J. & Falk, G. W. Predictors of Progression to High-Grade Dysplasia or Adenocarcinoma in Barrett's Esophagus. *Gastroenterol. Clin. North Am.***44**, 299–315 (2015).
  20. Read, M. D., Krishnadath, K. K., Clemons, N. J. & Phillips, W. A. Preclinical models for the study of barrett's carcinogenesis. *Ann. N. Y. Acad. Sci.***1434**, 139–148 (2018).
  21. Contino, G., Vaughan, T. L., Whiteman, D. & Fitzgerald, R. C. The Evolving Genomic Landscape of Barrett's Esophagus and Esophageal Adenocarcinoma. *Gastroenterology***153**, 657-673.e1 (2017).
  22. Integrated genomic characterization of oesophageal carcinoma. *Nature***541**, 169–175 (2017).
  23. Nowicki-Osuch, K. *et al.* Molecular phenotyping reveals the identity of Barrett's esophagus and its malignant transition. *Science***373**, 760–767 (2021).
  24. Sharma, P. *et al.* Dysplasia and cancer in a large multicenter cohort of patients with Barrett's esophagus. *Clin. Gastroenterol. Hepatol. Off. Clin. Pract. J. Am. Gastroenterol. Assoc.***4**, 566–572 (2006).
  25. Qureshi, A. P., Stachler, M. D., Haque, O. & Odze, R. D. Biomarkers for Barrett's esophagus—a contemporary review. *Expert Rev. Mol. Diagn.***18**, 939–946 (2018).
  26. Bansal, A. & Fitzgerald, R. C. Biomarkers in Barrett's Esophagus: Role in Diagnosis, Risk Stratification, and Prediction of Response to Therapy. *Gastroenterol. Clin. North Am.***44**, 373–390 (2015).
  27. Lopes, C. A. M. *et al.* Centrosome amplification arises before neoplasia and increases upon p53 loss in tumorigenesis. *J. Cell Biol.***217**, 2353–2363 (2018).
  28. Zhang, X. *et al.* Malignant transformation of non-neoplastic Barrett's epithelial cells through well-defined genetic manipulations. *PLoS One***5**, 1–11 (2010).
  29. Zhang, Q. *et al.* Acidic Bile Salts Induce Epithelial to Mesenchymal Transition via VEGF Signaling in Non-Neoplastic Barrett's Cells. *Gastroenterology***156**, 130-144.e10 (2019).
  30. Bettencourt-Dias, M. & Glover, D. M. Centrosome biogenesis and function: Centrosomics brings new understanding. *Nat. Rev. Mol. Cell Biol.***8**, 451–463 (2007).
  31. Nigg, E. A. & Raff, J. W. Centrioles, Centrosomes, and Cilia in Health and Disease. *Cell***139**, 663–678 (2009).
  32. Scheer, U. Historical roots of centrosome research: Discovery of Boveri's microscope slides in Würzburg. *Philos. Trans. R. Soc. B Biol. Sci.***369**, (2014).
  33. Sathanathan, A. H., Ratnasooriya, W. D., Silva, A. de & Randeniya, P. Rediscovering Boveri's centrosome in *Ascaris* (1888): its impact on human fertility and development. *Reprod. Biomed. Online***12**, 254–270 (2006).
  34. Lin, M., Xie, S. S. & Chan, K. Y. An updated view on the centrosome as a cell cycle regulator. *Cell Div.***17**, 1 (2022).
  35. Chan, J. Y. A Clinical Overview of Centrosome Amplification in Human Cancers. *Int. J.*

- Biol. Sci.***7**, 1122–1144 (2011).
36. Godinho, S. A., Kwon, M. & Pellman, D. Centrosomes and cancer: How cancer cells divide with too many centrosomes. *Cancer Metastasis Rev.***28**, 85–98 (2009).
  37. Song, S., Jung, S. & Kwon, M. Expanding roles of centrosome abnormalities in cancers. *BMB Rep.***56**, 216–224 (2023).
  38. Godinho, S. A. & Pellman, D. Causes and consequences of centrosome abnormalities in cancer. *Philos. Trans. R. Soc. B Biol. Sci.***369**, (2014).
  39. Dammermann, A. *et al.* Centriole assembly requires both centriolar and pericentriolar material proteins. *Dev. Cell***7**, 815–829 (2004).
  40. Holland, A. J., Lan, W. & Cleveland, D. W. Centriole duplication: A lesson in self-control. *Cell Cycle***9**, 2803–2808 (2010).
  41. Azimzadeh, J. & Bornens, M. Structure and duplication of the centrosome. *J. Cell Sci.***120**, 2139–2142 (2007).
  42. O'Connell, K. F. *et al.* The *C. elegans* zyg-1 Gene Encodes a Regulator of Centrosome Duplication with Distinct Maternal and Paternal Roles in the Embryo. *Cell***105**, 547–558 (2001).
  43. Wang, M. *et al.* Rab11-FIP1/RCP Functions as a Major Signalling Hub in the Oncogenic Roles of Mutant p53 in Cancer. *Mol. Biol. Cell***11**, 811–819 (2021).
  44. Gönczy, P. Centrosomes and cancer: Revisiting a long-standing relationship. *Nat. Rev. Cancer***15**, 639–652 (2015).
  45. Loncarek, J. & Bettencourt-Dias, M. Building the right centriole for each cell type. *J. Cell Biol.***217**, 823–835 (2018).
  46. Nigg, E. A. & Holland, A. J. Once and only once: mechanisms of centriole duplication and their deregulation in disease. *Nat. Rev. Mol. Cell Biol.***19**, 297–312 (2018).
  47. Arquint, C. & Nigg, E. A. The PLK4-STIL-SAS-6 module at the core of centriole duplication. *Biochem. Soc. Trans.***44**, 1253–1263 (2016).
  48. Habedanck, R., Stierhof, Y. D., Wilkinson, C. J. & Nigg, E. A. The Polo kinase Plk4 functions in centriole duplication. *Nat. Cell Biol.***7**, 1140–1146 (2005).
  49. Kim, D. H. *et al.* Cep131 overexpression promotes centrosome amplification and colon cancer progression by regulating Plk4 stability. *Cell Death Dis.***10**, (2019).
  50. Zhao, J. Z., Ye, Q., Wang, L. & Lee, S. C. Centrosome amplification in cancer and cancer-associated human diseases. *Biochim. Biophys. Acta - Rev. Cancer***1876**, 188566 (2021).
  51. Wang, P. *et al.* Type 2 Diabetes Promotes Cell Centrosome Amplification via AKT-ROS-Dependent Signalling of ROCK1 and 14-3-3 $\sigma$ . *Cell. Physiol. Biochem.***47**, 356–367 (2018).
  52. Mittal, K. *et al.* Hypoxia-induced centrosome amplification underlies aggressive disease course in hpv-negative oropharyngeal squamous cell carcinomas. *Cancers (Basel)***12**, 1–18 (2020).
  53. Basto, R. *et al.* Centrosome amplification can initiate tumorigenesis in flies. *Cell***133**, 1032–1042 (2008).

54. Godinho, S. A. *et al.* Oncogene-like induction of cellular invasion from centrosome amplification. *Nature***510**, 167–171 (2014).
55. Kazazian, K. *et al.* Plk4 Promotes Cancer Invasion and Metastasis through Arp2/3 Complex Regulation of the Actin Cytoskeleton. *Cancer Res.***77**, 434–447 (2017).
56. Mittal, K. *et al.* Centrosome amplification: a quantifiable cancer cell trait with prognostic value in solid malignancies. *Cancer Metastasis Rev.***40**, 319–339 (2021).
57. Prakash, A. *et al.* “Centrosome Amplification promotes cell invasion via cell-cell contact disruption and Rap-1 activation.” *bioRxiv* 2022.05.09.490051 (2022) doi:10.1242/jcs.261150.
58. Kayser, G. *et al.* Numerical and structural centrosome aberrations are an early and stable event in the adenoma–carcinoma sequence of colorectal carcinomas. *Virchows Arch.***447**, 61–65 (2005).
59. Ogden, A., Rida, P. C. G. & Aneja, R. Prognostic value of CA20, a score based on centrosome amplification associated genes, in breast tumors. *Sci. Rep.***7**, 1–11 (2017).
60. Mark Gustafson, L. *et al.* Centrosome Hyperamplification in Head and Neck Squamous Cell Carcinoma: A Potential Phenotypic Marker of Tumor Aggressiveness. *Laryngoscope***110**, 1798–1801 (2000).
61. Piemonte, K. M., Anstine, L. J. & Keri, R. A. Centrosome Aberrations as Drivers of Chromosomal Instability in Breast Cancer. *Endocrinology***162**, (2021).
62. LoMastro, G. M. & Holland, A. J. The Emerging Link between Centrosome Aberrations and Metastasis. *Dev. Cell***49**, 325–331 (2019).
63. Wu, Q., Li, B., Liu, L., Sun, S. & Sun, S. Centrosome dysfunction: a link between senescence and tumor immunity. *Signal Transduct. Target. Ther.***5**, (2020).
64. Kalkan, B. M., Ozcan, S. C., Quintyne, N. J., Reed, S. L. & Acilan, C. Keep Calm and Carry on with Extra Centrosomes. *Cancers (Basel)***14**, (2022).
65. Krämer, A. *et al.* Centrosome aberrations as a possible mechanism for chromosomal instability in non-Hodgkin’s lymphoma. *Leukemia***17**, 2207–2213 (2003).
66. Arnandis, T. *et al.* Oxidative Stress in Cells with Extra Centrosomes Drives Non-Cell-Autonomous Invasion. *Dev. Cell***47**, 409–424.e9 (2018).
67. Adams, S. D. *et al.* Centrosome amplification mediates small extracellular vesicle secretion via lysosome disruption. *Curr. Biol.***31**, 1403–1416.e7 (2021).
68. Pannu, V. *et al.* Rampant centrosome amplification underlies more aggressive. **6**, (2015).
69. Fukasawa, K. Centrosome amplification, chromosome instability and cancer development. *Cancer Lett.***230**, 6–19 (2005).
70. Cardoso, J. *et al.* CYR61 and TAZ Upregulation and Focal Epithelial to Mesenchymal Transition May Be Early Predictors of Barrett’s Esophagus Malignant Progression. *PLoS One***11**, (2016).
71. Caspa Gokulan, R., Garcia-Buitrago, M. T. & Zaika, A. I. From genetics to signaling pathways: molecular pathogenesis of esophageal adenocarcinoma. *Biochim. Biophys. acta. Rev. cancer***1872**, 37–48 (2019).
72. Rivera-Rivera, Y. *et al.* The Nek2 centrosome-mitotic kinase contributes to the

- mesenchymal state, cell invasion, and migration of triple-negative breast cancer cells. *Sci. Rep.***11**, 9016 (2021).
73. Kalluri, R. *et al.* The basics of epithelial-mesenchymal transition. *Phys. Plasmas***To be** **subm**, 1420–1428 (2010).
  74. Yeung, K. T. & Yang, J. Epithelial-mesenchymal transition in tumor metastasis. *Mol. Oncol.***11**, 28–39 (2017).
  75. Chen, T., You, Y., Jiang, H. & Wang, Z. Z. Epithelial-mesenchymal transition (EMT): A biological process in the development, stem cell differentiation, and tumorigenesis. *J. Cell. Physiol.***232**, 3261–3272 (2017).
  76. Rhys, A. D. *et al.* Loss of E-cadherin provides tolerance to centrosome amplification in epithelial cancer cells. *J. Cell Biol.***217**, 195–209 (2018).
  77. Liao, Z. *et al.* High PLK4 expression promotes tumor progression and induces epithelial-mesenchymal transition by regulating the Wnt/ $\beta$ -catenin signaling pathway in colorectal cancer. *Int. J. Oncol.***54**, 479–490 (2019).
  78. Satelli, A. & Li, S. Vimentin in cancer and its potential as a molecular target for cancer therapy. *Cell. Mol. Life Sci.***68**, 3033–3046 (2011).
  79. Kuburich, N. A., den Hollander, P., Pietz, J. T. & Mani, S. A. Vimentin and cytokeratin: Good alone, bad together. *Semin. Cancer Biol.***86**, 816–826 (2022).
  80. Fuyuhiko, Y. *et al.* Clinical significance of vimentin-positive gastric cancer cells. *Anticancer Res.***30**, 5239–5243 (2010).
  81. Wei, J. *et al.* Overexpression of vimentin contributes to prostate cancer invasion and metastasis via src regulation. *Anticancer Res.***28**, 327–334 (2008).
  82. Kidd, M. E., Shumaker, D. K. & Ridge, K. M. The role of Vimentin intermediate filaments in the progression of lung cancer. *Am. J. Respir. Cell Mol. Biol.***50**, 1–6 (2014).
  83. Moinova, H. *et al.* Aberrant vimentin methylation is characteristic of upper gastrointestinal pathologies. *Cancer Epidemiol. Biomarkers Prev.***21**, 594–600 (2012).
  84. Usman, S. *et al.* Vimentin is at the heart of epithelial mesenchymal transition (Emt) mediated metastasis. *Cancers (Basel)***13**, 1–26 (2021).
  85. Leppänen, J. *et al.* Tenascin-C and fibronectin in normal esophageal mucosa, Barrett's esophagus, dysplasia and adenocarcinoma. *Oncotarget***8**, 66865–66877 (2017).
  86. Spada, S., Tocci, A., Di Modugno, F. & Nisticò, P. Fibronectin as a multiregulatory molecule crucial in tumor matrix: from structural and functional features to clinical practice in oncology. *J. Exp. Clin. Cancer Res.***40**, 102 (2021).
  87. Pankov, R. & Yamada, K. M. Fibronectin at a glance. *J. Cell Sci.***115**, 3861–3863 (2002).
  88. Lin, T. C. *et al.* Fibronectin in cancer: Friend or foe. *Cells***9**, 1–37 (2020).
  89. Gopal, S. *et al.* Fibronectin-guided migration of carcinoma collectives. *Nat. Commun.***8**, 14105 (2017).
  90. Efthymiou, G. *et al.* Shaping Up the Tumor Microenvironment With Cellular Fibronectin. *Front. Oncol.***10**, 1–18 (2020).
  91. Xiao, J. *et al.* Expression of fibronectin in esophageal squamous cell carcinoma and its role in migration. *BMC Cancer***18**, 976 (2018).

92. Armstrong, H. K. *et al.* Dysregulated fibronectin trafficking by Hsp90 inhibition restricts prostate cancer cell invasion. *Sci. Rep.***8**, 2090 (2018).
93. Kenny, H. A. *et al.* Mesothelial cells promote early Ovarian cancer metastasis through fibronectin secretion. *J. Clin. Invest.***124**, 4614–4628 (2014).
94. Rick, J. W. *et al.* Fibronectin in malignancy: Cancer-specific alterations, protumoral effects, and therapeutic implications. *Semin. Oncol.***46**, 284–290 (2019).
95. De Oliveira Ramos, G. *et al.* Fibronectin modulates cell adhesion and signaling to promote single cell migration of highly invasive oral squamous cell carcinoma. *PLoS One***11**, 1–18 (2016).
96. Palanca-Wessels, M. C. A. *et al.* Extended lifespan of Barrett's esophagus epithelium transduced with the human telomerase catalytic subunit: A useful in vitro model. *Carcinogenesis***24**, 1183–1190 (2003).
97. Gomes, I. S. Impact of early centrosome deregulation in malignant transformation. (Universidade de Lisboa, Faculdade de Ciências (unpublished Master Thesis)).
98. Justus, C. R., Marie, M. A., Sanderlin, E. J. & Yang, L. V. Transwell In Vitro Cell Migration and Invasion Assays. *Methods Mol. Biol.***2644**, 349–359 (2023).
99. Kröger, C. *et al.* Acquisition of a hybrid E/M state is essential for tumorigenicity of basal breast cancer cells. *Proc. Natl. Acad. Sci. U. S. A.***116**, 7353–7362 (2019).
100. Moreno-Marin, N. *et al.* High prevalence and dependence of centrosome clustering in mesenchymal tumors and leukemia. *bioRxiv* 2023.03.13.532472 (2023) doi:10.1101/2023.03.13.532472.
101. Jovov, B. *et al.* Role of E-cadherin in the pathogenesis of gastroesophageal reflux disease. *Bone***17**, 211–224 (2009).
102. Das, L. Epigenetic alterations impede epithelial-mesenchymal transition by modulating centrosome amplification and Myc/RAS axis in triple negative breast cancer cells. *Sci. Rep.***13**, 1–17 (2023).
103. Dalton, C. J. & Lemmon, C. A. Fibronectin: Molecular Structure, Fibrillar Structure and Mechanochemical Signaling. *Cells***10**, (2021).
104. Ghura, H. *et al.* Inhibition of fibronectin accumulation suppresses tumor growth. *Neoplasia***23**, 837–850 (2021).
105. Yousif, N. G. Fibronectin promotes migration and invasion of ovarian cancer cells through up-regulation of FAK-PI3K/Akt pathway. *Cell Biol. Int.***38**, 85–91 (2014).
106. Jia, D., Entersz, I., Butler, C. & Foty, R. A. Fibronectin matrix-mediated cohesion suppresses invasion of prostate cancer cells. *BMC Cancer***12**, 94 (2012).
107. Fonseca I, Horta C, Ribeiro AS, Sousa B, Marteil G, Bettencourt-Dias M, P. J. Polo-like kinase 4 (Plk4) potentiates anoikis-resistance of p53KO mammary epithelial cells by inducing a hybrid EMT phenotype. *Cell Death Dis.* (2023) doi:10.1038/s41419-023-05618-1.
108. Garvey, D. R., Chhabra, G., Ndiaye, M. A. & Ahmad, N. Role of polo-like kinase 4 (PLK4) in epithelial cancers and recent progress in its small molecule targeting for cancer management. *Mol. Cancer Ther.***20**, 632–640 (2021).
109. Yamamoto, S. & Kitagawa, D. Emerging insights into symmetry breaking in centriole duplication: updated view on centriole duplication theory. *Curr. Opin. Struct. Biol.***66**, 8–

14 (2021).

110. Singh, C. K. *et al.* PLK4 is upregulated in prostate cancer and its inhibition reduces centrosome amplification and causes senescence. *Prostate***82**, 957–969 (2022).
111. Bajpai, M. *et al.* Repeated exposure to acid and bile selectively induces colonic phenotype expression in a heterogeneous Barrett's epithelial cell line. *Lab. Investig.***88**, 643–651 (2008).
112. Amrutkar, M., Aasrum, M., Verbeke, C. S. & Gladhaug, I. P. Secretion of fibronectin by human pancreatic stellate cells promotes chemoresistance to gemcitabine in pancreatic cancer cells. *BMC Cancer***19**, 596 (2019).
113. Varadaraj, A. *et al.* TGF- $\beta$  triggers rapid fibrillogenesis via a novel T $\beta$ RII-dependent fibronectin-trafficking mechanism. *Mol. Biol. Cell***28**, 1195–1207 (2017).
114. Mohrmann, K. & van der Sluijs, P. Regulation of membrane transport through the endocytic pathway by rabGTPases. *Mol. Membr. Biol.***16**, 81–87 (1999).
115. Homma, Y., Hiragi, S. & Fukuda, M. Rab family of small GTPases: an updated view on their regulation and functions. *FEBS J.***288**, 36–55 (2021).
116. Tang, Q. *et al.* Rab11-FIP1 mediates epithelial-mesenchymal transition and invasion in esophageal cancer. *EMBO Rep.***22**, 1–12 (2021).
117. Hehnlly, H., Chen, C.-T., Powers, C. M., Liu, H.-L. & Doxsey, S. The centrosome regulates the Rab11- dependent recycling endosome pathway at appendages of the mother centriole. *Curr. Biol.***22**, 1944–1950 (2012).